Wisecr: Secure Simultaneous Code Dissemination to Many Batteryless Computational RFID Devices

Yang Su, Michael Chesser, Yansong Gao, Alanson P. Sample and Damith C. Ranasinghe

Abstract—Emerging ultra-low-power tiny scale computing devices in Cyber-Physical Systems run on harvested energy, are intermittently powered, have limited computational capability, and perform sensing and actuation functions under the control of a dedicated firmware operating without the supervisory control of an operating system. Wirelessly updating or patching firmware of such devices is inevitable. We consider the challenging problem of simultaneous and secure firmware updates or patching for a typical class of such devices—Computational Radio Frequency Identification (CRFID) devices. We propose Wisecr, the first secure and simultaneous wireless code dissemination mechanism to multiple devices that prevents malicious code injection attacks and intellectual property (IP) theft, whilst enabling remote attestation of code installation. Importantly, Wisecr is engineered to comply with existing ISO compliant communication protocol standards employed by CRFID devices and systems. We comprehensively evaluate Wisecr's overhead, demonstrate its implementation over standards compliant protocols, analyze its security and implement an end-to-end realization with popular CFRID devices—the open-source code is released on GitHub.

I. Introduction

The maturation of energy-harvesting technology and ultralow-power compute systems is leading to the advent of intermittently-powered, batteryless devices that operate entirely on energy extracted from the ambient environment [1]. The batteryless, low cost simplicity and the maintenance free perpetual operational life of these *tiny scale* computing platforms provide a compelling proposition for edge devices in the Internet of Things (IoT) and Cyber-Physical Systems.

Recent developments of *tiny scale* computing devices such as WISP [2], MOO [3] and Farsens Pyros [4], or so called *Computational Radio Frequency Identification* (CRFID) devices, are highly resource limited, intermittently-powered, batteryless and operate on harvested RF (radio-frequency) energy. In particular, these devices are more preferable in scenarios that are challenging for traditional battery-powered sensors, for example, pacemaker control and implanted blood glucose monitoring [5] as well as domains where batteries are undesirable, for example, wearables for healthcare applications [6].

Despite various embodiments, the fundamental architecture of those devices include: microcontrollers, sensors, transceivers, and, at times actuators, with the most significant component, the *code* or software imparting the devices with the ability to communicate and realize interactive tasks [7], [8]. Consequently, the update and patching of this firmware is inevitable. In the absence of standard protocols or system level support, firmware is typically updated using a wired

programming interface [3], [9]. However, in a practical application context, especially where devices are deeply embedded, the traditional method of updates are impractical or often impossible. Further, the wired interface results in a potential attack vector to tamper with the behavior of the devices [10] and a compromised device can be further hijacked to attack other networked entities [11].

The recent *Stork* [12] protocol addressed the challenging problem of fast wireless firmware updates to multiple CRFID devices. However, as illustrated in Fig. 1, *Stork* allows any party, authorized or not, armed with a simple RFID reader to: i) mount malicious code injection attacks; ii) tamper with device behaviour; and iii) steal intellectual property (IP) by simply eavesdropping on the over-the-air communication channel. Although a recent protocol [13] addressed the problem of malicious code injection attacks where by a single CRFID device is updated in turn, it neither supports simultaneous updates to many devices nor protects firmware IP and lacks a mechanism to validate the installation of code on a device.

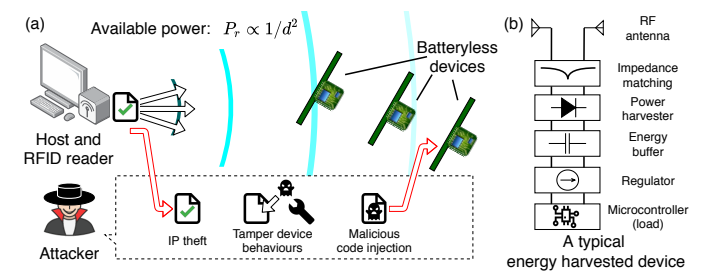


Fig. 1. (a) An Attacker may commit i) IP theft, ii) tamper with device behaviour, and iii) inject malicious code over the non-secure channel. (b) A typical device architecture where the amount of power available for harvesting decreases exponentially with distance d from a powering source.

Why Secure Wireless Firmware Update is Challenging?

Constructing a secure wireless firmware update mechanism for ultra-low power and batteryless devices is non-trivial; designing a secure method is challenged by: i) (C1) limited and indeterminate powering; i) (C2) unavailability of hardware security support; iii) (C3) constrained air interface protocols; iv) (C4) unavailability of supervisory control from an operating system. We elaborate on the challenges below.

C1. Energy-harvesting systems operate intermittently, only when energy is available from the environment. To operate, a device gradually buffers energy into a storage element (capacitor). Once sufficient energy is accumulated, the device begins operations. However, energy depletes more rapidly (e.g. milliseconds) during an operation compared to energy accumulation/charging (e.g. seconds). Further, energy accumulation in RF energy harvesting is sacrificed in backscatter communication links since a portion of the incident energy is reflected back during communications. Therefore, *power*

Y. Su, M. Chesser and D. C. Ranasinghe are with Auto-ID Lab, School of Computer Science, The University of Adelaide, Australia. (yang.su01, michael.chesser, damith.ranasinghe)@adelaide.edu.au

Y. Gao is with CSIRO's Data61, Australia. garrison.gao@data61.csiro.au A. P. Sample is with Electrical Engineering and Computer Science, University of Michigan, USA. apsample@umich.edu

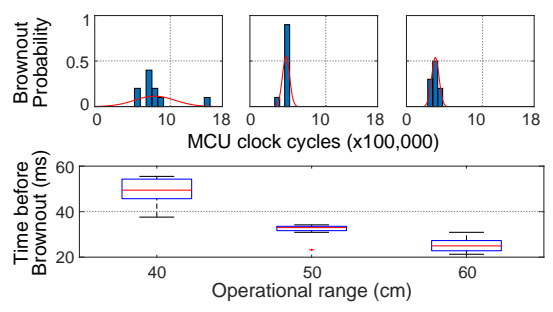


Fig. 2. The distribution of available clock cycles (top) and corresponding time (bottom) before *brownout*—exhaustion of available energy under computational load—for the open hardware and open software CRFID, WISP5.1LRG [9] built with a MSP430 microcontroller. We executed a message authentication code as the computational load and the device location is increased from 40 cm to 60 cm above a powering source—RFID reader antenna. We can observe that available MCU clock cycles and operational time periods before state loss are limited per charging-brownout cycle.

failures are common and occur in millisecond time scales [12], [14], [15] as experimentally validated in Fig. 2.

Timing of power loss events across devices are ad-hoc. For example, harvested energy varies under differing distances; therefore, a computation task may only execute partially before power failure and its hard to predict when it will occur. Further, saving and subsequently retrieving state at code execution checkpoints for a long-run application via an intermittent execution model [16] is not only: i) costly in terms of computations and energy [17]—saving state in non-volatile memories such as FLASH or EEPROM consumes more energy than static RAM (SRAM) whilst reading state from FRAM consumes more energy than writing as we demonstrate in Fig. 5; but also: ii) render a device in a vulnerable state for an attacker to exploit when checkpoint state is stored on off-chip memory with an easily accessible memory bus [18]. These issues make the execution of long-run security algorithms, such as Elliptic Curve Diffie-Hellman (ECDH)¹ key exchange, difficult to deploy securely. Consequently, power must be carefully managed to avoid power loss and leaving the device in a potentially vulnerable state; and, we must seek computationally efficient security schemes.

C2. Highly resource-constraint devices lack hardware security support. Thus, security features, including a trusted execution environment (TEE)—for example, ARM Trustzone [21]—and dedicated memory to explicitly maintain the secrecy of a long term secret keys, as in [22], are unavailable.

C3. The widely used wireless protocol for UHF (Ultra High Frequency) RFID communication only provides *insecure unicast communication links* and supports no broadcast features or device-to-device communication possible in mesh networking typical of wireless sensor networks.

¹We are aware of optimized public key exchange implementations such as ECDH and Ring-LWE [19], [20]; however, they are impractical for passively powered resource-constrained devices. For example, ECDH [19] with Curve25519 still requires 4.88 million clock cycles on a MSP430 MCU. In contrast, there are a very limited number of clock cycles available from harvested-energy before energy depletion [13], [14]—e.g. 400,000 clock cycles expected even at close proximity of 50 cm from an energy source, see Fig. 2—and there is very limited time available for computations where a CRFID must reply before strict air interface protocol time-outs are breached.

C4. Unlike wireless sensor network nodes, severely resource limited systems, such as CRFID, do not operate under the supervisory control of an operating system to provide security or installation support for a secure dissemination scheme.

A. Our Study

We consider the problem of secure and simultaneous code dissemination to multiple RF-powered CRFID devices operating under constrained protocols, device capability, and extreme on-device resource limitations—computing power, memory, and energy. The scheme we developed overcomes the unique challenges, protects the firmware IP during the dissemination process, prevents malicious code injection attacks and enables remote attestation of code installation. More specifically, we address the following security threats:

- Malicious code injection: code alteration, loading unauthorized code, loading code onto an unauthorized device, and code downgrading.
- Incomplete firmware installation
- IP theft: reverse engineering from plaintext binaries.

Consequently, we fulfil the *urgent* and *unmet* security needs in the existing state-of-the-art multiple CRFID wireless dissemination protocol—Stork [12].

B. Our Contributions and Results

Contribution 1 (Section II)—Wisecr is the first secure and simultaneous (fast) firmware dissemination scheme to multiple batteryless CRFID devices. Wisecr provides three security functions for secure and fast updates: i) preventing malicious code injection attacks; ii) IP theft; and iii) attestation of code installation. Wisecr achieves rapid updates by supporting simultaneous update to multiple CRFID devices through a secure broadcasting of firmware over a standard non-secure unicast air interface protocol

Contribution 2 (Section III & IV-A)—A holistic design trajectory, from a formal secure scheme design to an end-to-end implementation requiring only limited on-device resources. Ultra-low power operating conditions and on-device resource limitations demand both a secure and an efficient scheme. First, we built an efficient broadcast session key exchange exploiting commonly available hardware acceleration for crypto on microcontroller units (MCUs).

Second, to avoid power loss and thus achieve uninterrupted execution of a firmware update session, we propose *new* methods: i) adaptive control of the execution model of devices using RF powering channel state information collected and reported by field deployed devices; ii) reducing disruptions to broadcast data synchronisation across multiple devices by introducing the concept of a *pilot tag* selection from participating devices in the update scheme to drive the protocol. These methods avoid the need for costly, secure checkpointing methods and leaving a device in a vulnerable state during power loss.

Third, in the absence of an operating system, we develop an immutable bootloader to: i) supervise the control flow of the secure firmware update process; ii) minimize the occurrence of power loss during an update session whilst abandoning

a session in case an unpreventable power loss still occurs; and iii) manage the secure storage of secrets by exploiting commonly available on-chip memory protection units (MPUs) to realize an immutable, bootloader-only accessible, secrets.

Contribution 3 (Section IV-A, Supplementary Material (Supp. Material) S I to S III)—Standards compliant end-to-end Wisecr implementation. We develop Wisecr from specification, component design to architecture on the device, and implementation. We evaluate Wisecr extensively, including comparisons with current non-secure methods, and validate our scheme by an end-to-end implementation with an open source code release on GitHub: https://github.com/ AdelaideAuto-IDLab/Wisecr. Wisecr is a standard compliant secure firmware broadcast mechanism with a demonstrable implementation using the widely adopted air interface protocol— ISO-18000-63 protocol albeit the protocol's lack of support for broadcasting or multi-casting—and using commodity devices from vendors. Hence, the Wisecr scheme can be adopted in currently deployed systems. We demonstrate the firmware dissemination process here https://youtu.be/'OuStZsTyV8.

Paper Organisation. Section II presents the threat model, security requirements and Wisecr design; Section III details how the demanding security requirements are met under challenging settings; Section IV-A discusses our end-to-end implementation, followed by performance and security evaluation of Wisecr and its end-to-end implementation in Section IV; Section V discusses related work with which Wisecr is compared. Section VI concludes this work.

II. Wisecr DESIGN

In this section, we describe the threat model including a summary of notations in Table I, followed by details of *Wisecr* design, and then proceed to identify the minimal hardware security requirements needed to implement the scheme.

A. Threat Model

Communication with an RFID device operating in the UHF range is governed by the widely adopted ISO-18000-63—also known as the EPCglobal Class 1 Generation 2 version 2 (C1G2v2)—air interface protocol or simply the *EPC Gen2*.

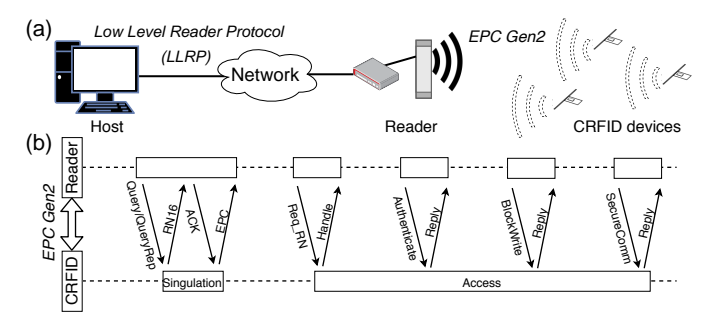


Fig. 3. (a) System overview. (b) Control/data flow over the *EPC Gen2* air interface. Firmware update will take place once a device enters the *Access* state and by implementing *Wisecr* over *Access* command specifications such as Authenticate.

TABLE I. Table of Notations

| DB | Server's database, where each element is a three-tuple de- | | | | | |
|--------------------------|---|--|--|--|--|--|
| DD | scribing each CRFID token: i) the unique and immutable | | | | | |
| | identification number id ; ii) the device specific secret key k ; | | | | | |
| | and iii) a flag denoting a device requiring an update valid. | | | | | |
| firmware | The new firmware binary for the update. | | | | | |
| | The new infinite contact for the update. The $j_{\rm th}$ block of the firmware. | | | | | |
| nver | The new version number (a monotonically increasing ordinal | | | | | |
| iivei | number with a one-to-one correspondence with each updated | | | | | |
| | firmware). | | | | | |
| ver | A token's current version number. | | | | | |
| sk | The broadcast session key. | | | | | |
| s | The MAC tag computed by the Server. | | | | | |
| \mathbf{c}, \mathbf{r} | Attestation challenge and response, respectively. | | | | | |
| ' | An apostrophe denotes a value computed by a different entity, | | | | | |
| | eg., s' the MAC tag computed by a Token. | | | | | |
| \square_i | A subscript i denotes a specific entity, e.g., \mathbf{k}_i is the device | | | | | |
| | key of the $i_{ m th}$ Token. | | | | | |
| $\langle \Box \rangle$ | Encrypted data, e.g. $\langle \mathbf{sk}_i \rangle$ denotes the encrypted session key | | | | | |
| | $\mathbf{s}\mathbf{k}$, with the i_{th} token's key \mathbf{k}_i . | | | | | |
| RNG() | A cryptographically secure random number generator. | | | | | |
| SKP.Enc() | Symmetric Key Primitive encryption function described by | | | | | |
| | $\langle \mathbf{m} \rangle \leftarrow SKP.Enc_{\mathbf{sk}}(\mathbf{m})$. Here, the plaintext \mathbf{m} is nen- | | | | | |
| OKED () | crypted with the \mathbf{sk} to produce the ciphertext $\langle \mathbf{m} \rangle$. | | | | | |
| SKP.Dec() | Symmetric Key Primitive decryption function where $\mathbf{m} \leftarrow$ | | | | | |
| N4AC() | $SKP.Dec_{\mathbf{sk}}(\langle \mathbf{m} \rangle).$ | | | | | |
| MAC() | Message Authentication Code function. By appending an | | | | | |
| | authentication tag s to the message m, where $s \leftarrow MAC_k(m)$, | | | | | |
| | a message authentication code (MAC) function can verify the integrity and authenticity of the message by using the | | | | | |
| | symmetric key \mathbf{k} . | | | | | |
| SNIFF() | Measures the voltage Vt_i established by the power harvester | | | | | |
| SIVIII I () | within a fixed time t from boot-up at token i , as $\mathbf{V}\mathbf{t}_i \leftarrow$ | | | | | |
| | SNIFF (t) . | | | | | |
| PAM() | Family of functions employed by the Power Aware Execution | | | | | |
| () | mode of operation proposed for the token to mitigate power- | | | | | |
| | loss (brown-out) events. | | | | | |
| Query | We denote <i>EPC Gen2</i> commands using typewriter fonts. | | | | | |

Fig. 3 illustrates the communication channels in a networked RFID system. The RFID reader resides at the edge of the network and is typically connected to multiple antennas to power and communicate with RFID or CRFID devices energized by the antennas. The reader network interface is accessed by using a Low-Level Reader Protocol (LLRP) from a host machine. Communication with an RFID device operating in the UHF range is through the *EPC Gen2* protocol.

Our focus is on the insecure communication channel between the RFID reader connected antenna and the CRFID transponder or token \mathcal{T} . Hence, we assume that the communication between a host and a reader is secured using standard cryptographic mechanisms [23]. Therefore, a host computer and a reader are considered as a single entity, the Server, denoted as \mathcal{S} (a detailed execution of an EPC Gen2 protocol session to singulate a single CRFID device from all visible devices in the field can be found in [12], [14]). Once devices are singulated, we employ the EPC Gen2 protocol commands supported in the device Access state to encapsulate the secure firmware update.

We assume a CRFID device can meet the pragmatic hardware security requirements, detailed in Section II-C. Further, after device provisioning, the wired interface for programming is disabled—using a common technique adopted to secure resource-constrained microcontroller based devices [13], [15]. Subsequently, both the trusted party and adversary $\mathcal A$ must use the wireless interface for installing new firmware on a token.

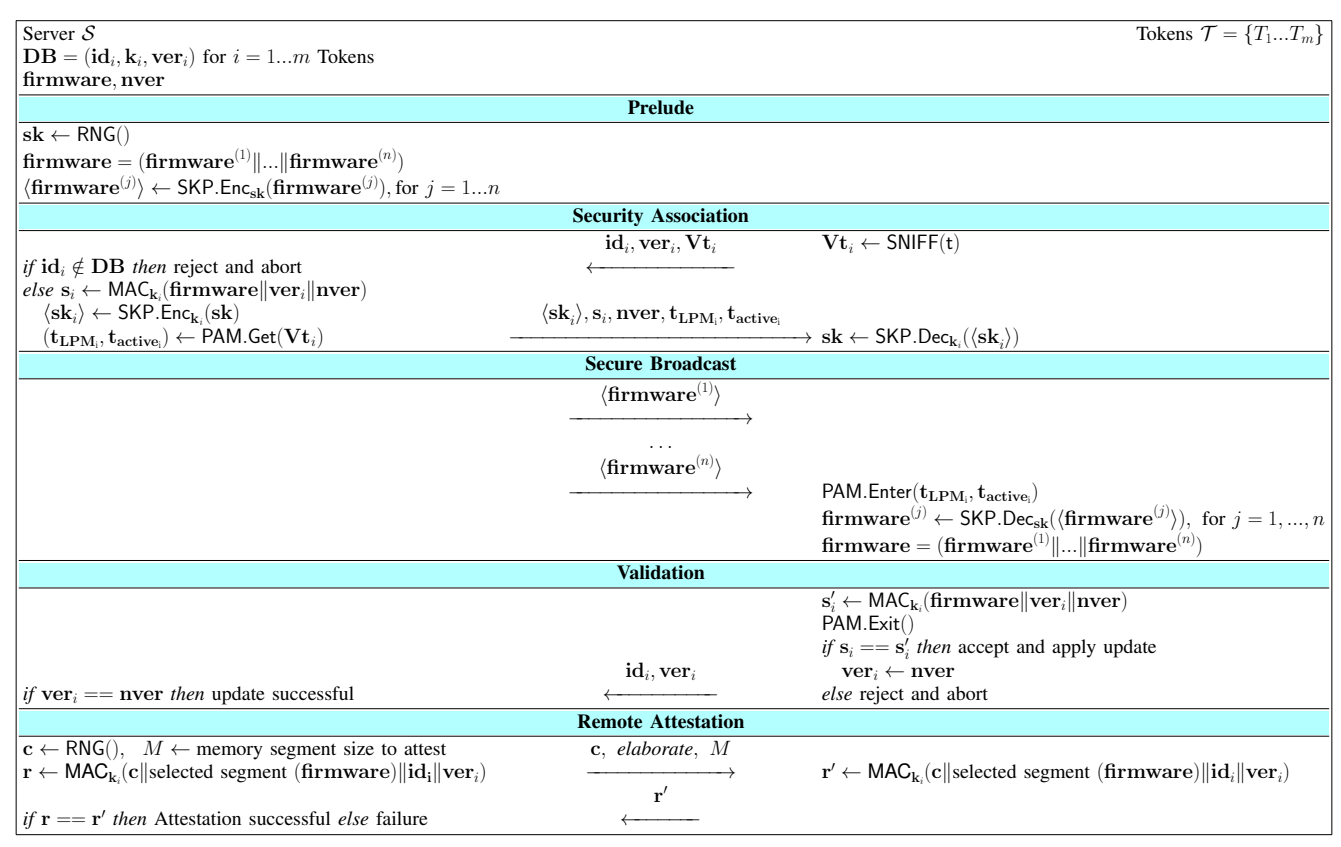


Fig. 4. Wisecr: The proposed wireless, secure and simultaneous code dissemination scheme to multiple tokens. Notably, the functions SNIFF() and PAM() facilitate the secure and uninterruptible execution of an update session. A single symmetric key cipher SKP can be exploited in practice to realise all of the primitives needed, including the MAC() function, to address the demands of a resource limited setting.

Building upon relevant adversary models related to wireless firmware update for low-end embedded devices [24], [25], we assume an adversary $\mathcal A$ has full control over the communication channel between the Server $\mathcal S$ and the token $\mathcal T$. Hence, the adversary $\mathcal A$ can eavesdrop, manipulate, record and replay all messages sent between the Server $\mathcal S$ and the token $\mathcal T$. This type of attacker is referred to as an input/output attacker in the model of Piessens and Verbauwhede [26].

Similar to [24], [25], we assume that the adversary cannot bypass any of the memory hardware protections (detailed in Section II-C) and cannot mount physical attacks to extract non-volatile memory contents. Such an assumption is practical, especially in deeply embedded applications such as pacemaker control [14] where wireless update is the only practical mechanism by which to alter the firmware and physical access is extremely difficult. As in [27], we also assume the adversary $\mathcal A$ cannot mount implementation attacks against the CRFID, or gain internal variables in registers, for example, using invasive attacks and side-channel analysis. We do not consider Denial of Service (DoS) attacks because it appears to be impossible to defend against such an attacker, for example, that disrupts or jams the wireless communication medium in practice [24].

B. Wisecr Update Scheme

Wisecr enables the ability to securely distribute and update the firmware of multiple CRFID tokens, simultaneously. Given that a Server S must communicate with an RFID device T using EPC Gen2, Wisecr is compatible with EPC Gen2

by design. Generally, our scheme can be implemented after the execution of the anti-collision algorithm in the media access control layer of the EPC Gen2 protocol, where a reader must first singulate a CRFID device and obtain a handle, RN16, to address and communicate with each specific device. After singulating a device, the server can employ the EPC Gen2 device Access commands, namely, BlockWrite, Authenticate, SecureComm and TagPrivilege specified in the EPC Gen2 to implement the Wisecr scheme. We describe the update scheme in Fig. 4 and defer the details of our scheme implemented over the EPC Gen2 protocol to the Supp. Material S II.

As described in Table I, the Server S maintains a database **DB** of provisioned tokens, issues the new **firmware** and the corresponding version number (**nver**). Each token T is provisioned with: i) an id_i , the immutable identification number; ii) k_i , the device specific secret key stored in NVM that is read-only accessible by the immutable bootloader; iii) ver_i , the token's current firmware version number stored in NVM that is write-only accessible by the immutable bootloader.

We describe a dissemination session in four stages: i) Prelude; ii) Security Association; iii) Secure Broadcast; and iv) Validation. An update can be extended with an optional, v) Remote Attestation to verify the firmware installation.

STAGE 1: Prelude (Offline). In this stage, the Server S undertakes setup tasks. The Server uses RNG() to generate a broadcast session key (sk). The new **firmware** is divided into segments—or block; each block j is en-

crypted as $\langle \mathbf{firmware}^{(j)} \rangle \leftarrow \mathsf{SKP.Enc_{sk}}(\mathbf{firmware}^{(j)})$, where $\langle \mathbf{firmware}^{(j)} \rangle$ denotes the encrypted firmware block j. The division of firmware is necessary as the narrow band communication channel and the $EPC\ Gen2$ protocol does not allow arbitrary size payloads to be transmitted to a token.

STAGE 2: Security Association. In this stage, the Server \mathcal{S} distributes the broadcast session key (\mathbf{sk}) to all tokens \mathcal{T} and builds a secure broadcast channel over which to simultaneously distribute the firmware to multiple tokens.

More specifically, each token in the energizing field of the Server responds with $i\mathbf{d}_i$, $V\mathbf{t}_i$ and $v\mathbf{er}_i$. The token will not be included in the following update session if: i) the $i\mathbf{d}_i$ of the responding token is not in Server's $D\mathbf{B}$; or ii) the token is not scheduled for an update ($vali\mathbf{d}_i == False$). For tokens selected for an update, the Server computes a MAC tag $\mathbf{s}_i \leftarrow \mathsf{MAC}_{\mathbf{k}_i}(\mathbf{firmware}||\mathbf{ver}_i||\mathbf{nver})$. In practice, we cannot assume that each token is executing the same version of the firmware, therefore a token specific MAC tag is generated over the device specific key whilst the firmware is encrypted with the broadcast session key.

The Server establishes a shared session key with each token T_i by sending $\langle \mathbf{sk}_i \rangle$, where $\langle \mathbf{sk}_i \rangle \leftarrow \mathsf{SKP.Enc}_{\mathbf{k}_i}(\mathbf{sk})$ and \mathbf{k}_i is specific to the i_{th} token, and \mathbf{nver} . The $\langle \mathbf{sk}_i \rangle$ and \mathbf{s}_i are transmitted to each token T_i . Each token decrypts the broadcast session key $\mathbf{sk} \leftarrow \mathsf{SKP.Dec}_{\mathbf{k}_i}(\langle \mathbf{sk}_i \rangle)$ —thus, all tokens selected for an update now possess the session key.

Notably, as detailed in Section III-B2, each token measures its powering channel state or its ability to harvest energy by measuring the voltage Vt_i established by the power harvester within a fixed time t from boot-up, as $Vt_i \leftarrow SNIFF(t)$ to transmit to the Server. There are two important reasons for measuring Vt_i . First, to facilitate the power-aware execution model (PAM) employed to mitigate power-loss at a given token. The Server uses the reported Vt_i to control the execution model of the $i_{\rm th}$ token. Specifically, the reported $\mathbf{V}\mathbf{t}_i$ is used by the Server to determine the length of time that a token dwells in low power mode (LPM) t_{LMP_i} and active mode t_{active_i} when executing computationally intensive tasks in the Secure Broadcast and Validation stages; here, the server determines $(t_{\text{LPM}_i}, t_{\text{active}_i}) \leftarrow \text{PAM.Get}(\mathbf{Vt}_i)$. Second, the Server uses the reported Vt_i to realize the *Pilot-Observer Mode* of operation where one token is *elected* based on its Vt_i , termed the *Pilot*, to control the flow in the Secure Broadcast stage by responding to server commands as detailed in Stage 3.

STAGE 3: Secure Broadcast. In this stage, the encrypted firmware blocks $\langle \text{firmware}^{(1..n)} \rangle$ are boradcasted; and each token stores the new encrypted firmware blocks in its application memory region (Segment M defined in Section III-A). Once the broadcast is completed, each token starts firmware decryption and validation. The $\langle \text{firmware} \rangle$ is decrypted using the session key sk as $\text{firmware}^{(j)} \leftarrow \text{SKP.Dec}_{sk}(\langle \text{firmware}^{(j)} \rangle)$.

To realize a secure and power efficient logical broadcast channel under severely energy constrained settings, we use the *Pilot-Observer Mode*. Herein, all tokens, except the *Pilot* token elected by the Server, enters into an *Observer Mode*. The tokens in the *Observer Mode* silently listens and stores encrypted

data disseminated by the server; the *Pilot* token performs the same operation whilst responding to the server commands. We employ two techniques within the Pilot Observer Mode to mitigate power-loss and to achieve a secure broadcast to tokens: i) disabling energy consuming communication command reply from Observers; and ii) the concept of electing a *Pilot* CRFID device to drive the update session as detailed in Section III-B2.

Notably, the techniques described in Stage 2 and 3 form the foundation for the uninterrupted execution of the bootloader to ensure security and enhance the performance of the firmware dissemination under potential power-loss events.

STAGE 4: Validation. In this stage, firmware is validated before installation. More precisely, a token specific MAC tag $\mathbf{s}_i' \leftarrow \mathsf{MAC_{k_i}}(\mathsf{firmware}||\mathbf{ver}_i||\mathbf{nver})$ is computed by each token T_i . If the received MAC tag \mathbf{s}_i matches the device computed \mathbf{s}_i' , the integrity of the firmware established and the issuing Server is authenticated by the token. Subsequently, the new firmware is updated and the new version number \mathbf{nver} is stored as \mathbf{ver}_i . Otherwise, the firmware is discarded and the session is aborted. At stage completion, each token switches from the *Observer* or *Pilot* to the normal mode of operation.

Once the firmware is installed, the Server is acknowledged with the status of each token that participated in the session. This is achieved by performing an EPC Gen2 handshake after a reboot of the tokens, and comparing the version number \mathbf{ver}_i reported from each token specified by \mathbf{id}_i to the new firmware version number \mathbf{nver} expected from the token. If the \mathbf{ver}_i is up-to-date, the Server is acknowledged that the token T_i has been successfully updated.

STAGE 5 (Optional): Remote Attestation. The Server can elect to verify the firmware installation on a token by performing a remote attestation; a mechanism for the Server to verify the complete and correct software installation on a token. Considering the highly resource limited tokens, we propose a lightweight challenge response based mechanism re-using the MAC() function developed for *Wisecr*. The server sends a randomly generated challenge $c \leftarrow \mathsf{RNG}()$ and evaluates the corresponding response r' to validate the installation.

We propose two modes of attestation; a *fast mode* and an *elaborate mode* to trade-off veracity of the verification against computational and power costs as detailed in Supp. Material S III. We illustrate (in Fig. 4) and demonstrate (in Section IV-D) the *elaborate* mode (more veracious and computationally intensive) where response $\mathbf{r}' \leftarrow \mathsf{MAC}_{\mathbf{k}_i}(\mathbf{c}||\mathbf{selected segment (firmware)}||\mathbf{id}_i||\mathbf{ver}_i)$ attests the application memory segment of size M containing the installed **firmware**. In contrast, the *fast* method computes the response as $\mathbf{r}' \leftarrow \mathsf{MAC}_{\mathbf{k}_i}(\mathbf{c}||\mathbf{id}_i||\mathbf{ver}_i)$.

C. Token Security Requirements and Functional Blocks

Our design is intentionally minimal and requires the following security blocks.

Immutable Bootloader (Section III-A) We require a static NVM sector $M_{\rm rx}$ that is write-protected to store the executable bootloader image.

Secure Storage (Section III-A) To store a device specific secret, e.g., \mathbf{k}_i , we require an NVM sector M read-only accessible by the immutable bootloader in sector $M_{\rm rx}$.

Uninterruptible Bootloader Execution (Section III-B) During the execution of the bootloader stored in sector $M_{\rm rx}$, execution cannot be interrupted until the control flow is intentionally released by the bootloader.

Efficient Security Primitives (Section III-C) The update scheme requires: i) a symmetric key primitive; and ii) a keyed hash primitive for the message authentication code that are both computationally and power efficient.

We discuss in Section III how these properties and associated functional blocks are engineered on typical RF-powered devices built with ultra-low power commodity MCUs.

III. On-device Security Function Engineering

In order to provide comprehensive evaluations and demonstration, we selected the WISP5.1-LRG [9] CRFID device with an open-hardware and software implementation for our token \mathcal{T} . This CRFID device uses the ultra-low power MCU MSP430FR5969 from Texas Instruments. Consequently, for a more concrete discussion, we will refer to the WISP5.1-LRG CRFID and the MSP430FR5969 MCU in the following.

A. Immutable Bootloader & Secure Storage

For resource limited MCUs, several mechanisms—detailed in the Supp. Material S I—exists for implementing secure storage: i) Isolated Segments; ii) Execute Only Memory; iii) Runtime Access Protection; and iv) Volatile Keys.

Here, we opt for achieving secure storage and bootloader immutability using Runtime Access Protection by exploiting the MCU's memory protection unit (MPU), which offers flexibility to the bootloader. In particular, the MPU allows read/write/execute permissions to be defined individually for memory segmentsat power-up—prior to any application code execution. Wisecr requires the following segment permissions to be defined by the bootloader to prevents their subsequent modifications through application code by locking the MPU:

Segment M is used as the secure storage area. During application execution, any access (reading/writing) to this segment results in an access violation, causing the device to restart in the bootloader.

Segment $M_{\rm rx}$ contains the bootloader, device IVT (interrupt vector table), shared code (e.g., *EPC Gen2* implementation). During application execution, writing to this segment results in an access violation.

Segment M_{rwx} covers the remaining memory, and is used for application IVT, code (**firmware**) and data.

B. Uninterruptible Bootloader Execution

The execution or control flow of the bootloader on the token must be uninterruptible by application code and power-loss events to meet our security objectives but dealing with brownout induced power-loss events is more challenging. Power loss leaves devices in vulnerable states for attackers to exploit; therefore, we focus on innovative, pragmatic and

low-overhead power-loss prevention methods. Our approach deliberately mitigates the chances of power-loss. In case a rare power-loss still occurs, the token will discard all state—including security parameters such as the broadcast session key; subsequently, the Server will re-attempt to update the firmware by re-commencing a fresh update session with this token. We detail our solution below.

1) Managing Application Layer Interruptions: The bootloader must be uninterruptible (by application code) for security considerations. For instance, the application code—due to an unintentional software bug or otherwise—could interrupt the bootloader while the device key is in a CPU register, so that the application code (exploited by an attacker) can copy the device key to a location under its control, or completely subvert access protections by overriding the MPU register before it is locked.

Recall, the memory segment $M_{\rm rx}$ (see Section III-A) includes the memory region containing the IVT. This ensures that only the bootloader can modify the IVT. Since the IVT is under the bootloader's control, we can ensure that any non-maskable interrupt is unable to be directly configured by the application code, whereas all other interrupts are disabled during bootloader execution. Consequently, the interrupt configuration cannot be mutated by application code.

2) Managing Power-Loss Interruptions: Frequent and inevitable power loss during the bootloader execution will not only interrupt the execution, degrading code dissemination performance but also compromise security. Although intermittent computing techniques relying on saving and retrieving state at check-points from NVM—such as FLASH or EPPROM—is possible, these methods impose additional energy consumption and introduce security vulnerabilities revealed recently [18].

Confronted with the complexity of designing and implementing an end-to-end scheme under extreme resource limitations, we propose an on-device Power Aware execution Model (PAM) to: i) avoid the overhead of intermittent computing techniques; and ii) enhance security without saving checkpoints to insecure NVM.

We observe that only a limited number of clock cycles are available for computations per charge and discharge cycle (Intermittent Power Cycle or IPC) of a power harvester, as illustrated via comprehensive measurements in Fig. 2. Further, the rate of energy consumption/depletion is faster than energy harvesting. We recognize that there are three main sources of power-loss: i) (CPU) energy required for function computation exceeding the energy supply capability from the harvester; ii) (FRAM.R/W) memory read/write access such as in executing Blockwrite commands; and iii) (RFID) power harvesting disruptions from communications—especially for backscattering data in response to *EPC Gen2* commands.

To understand the severity of these four causes, we measure the maximum time duration before brownout/power-loss versus the operational range for each task—CPU, FRAM.R, FRAM.W and RFID. The results are detailed in Fig. 5. For an operational range less than or equal to 40 cm, the CR-FID transponder continuously operates without power failure. Beyond this range, the average operating time of the RFID

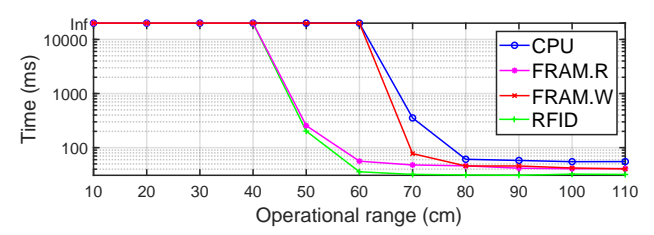


Fig. 5. Impact of four key device tasks on power-loss: CPU (computations); FRAM.R/W (memory read/write accesses); and RFID (communications). The data above are collected by using special firmware. The power-loss event is captured by monitoring through a GPIO pin. We conduct 10 repeated measurements and report the mean time before power-loss.

task drops rapidly from 40 cm. This is because the RFID communication process invokes shorting the antenna, during which the energy harvesting is interrupted. Notably, different from FLASH memory, reading data form FRAM (FRAM.R) consumes more power than writing to it (FRAM.W) as a consequence of the destructive read and the compulsory write-back [28]. The CPU task and the FRAM.W task can maintain continuous operation up to 60 cm, subsequently, these processes begin to brownout as the operational distance is increased further. Consequently, we developed:

- The Pilot-Observer Mode to reduce the occurrence of RFID tasks by enabling observing devices to listen to broadcast packets in silence whilst electing a single Pilot token to respond to the Server.
- The *Power Aware Execution Model (PAM)* to ensure memory access (FRAM tasks) and intensive computational blocks of the security protocol (CPU tasks) do not exceed the powering capability of the device.

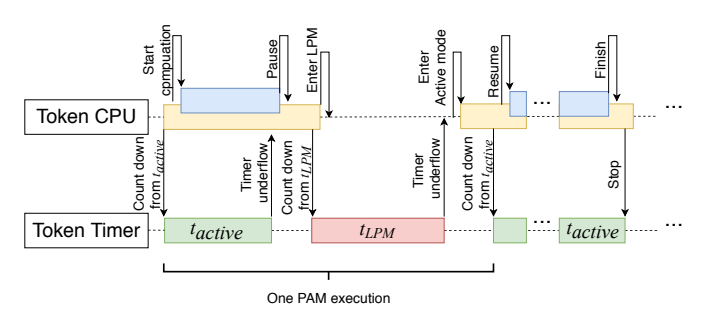


Fig. 6. A sequence diagram describing our proposed PAM and illustrating the interaction between the Token's CPU execution and the hardware timer. One PAM execution cycle consists of an active mode followed by a low power mode (LPM), one complete task may involve multiple PAM cycles.

Power Aware Execution Model (PAM). The execution mode enables a token to dynamically switch between *active* power mode and lower power mode (LPM)—LPM preserves (SRAM) state and avoids power-loss while executing a task. PAM is illustrated in Fig. 6. In active power mode, the token executes computations, and switches to LPM before power-loss to accumulate energy; subsequently, the token is awoken to active power mode to continue the previous computation after a period of $t_{\rm LPM}$.

Notably, our PAM model builds upon [13], [29] in that, these are designed for execution scheduling to *prevent power-loss from brownouts*. Compared to [13], we consider dynamic scheduling of tasks and in contrast to [29] sampling of the harvester voltage (*only possible in specific devices*) within the

application code, we consider dynamic scheduling determined by the more resourcefull Server \mathcal{S} using a single voltage measurement reported by a token \mathcal{T} (see Supp. Material S IV for detailed comparison). We outline the means of achieving our PAM model on a token below.

During the Security Association stage shown in Fig. 4, a token measures and reports the voltage $\mathbf{Vt}_i \leftarrow \mathsf{SNIFF}(t)$ to the Server. The \mathbf{Vt}_i measurement indicates energy that can be harvested by token i under the settings of the current firmware update session. According to \mathbf{Vt}_i , the Server determines the active time period t_{active} and LPM time period t_{LPM} for each CRFID device (detailed development of a model to estimate t_{active} and t_{LPM} from \mathbf{Vt} is in Supp. Material S \mathbf{V}). Consequently, each CRFID device's execution model is configured by the Server with device specific LPM and active periods at run-time. Hence, an adaptive execution model customised to the available power that could be harvested by each CRFID device is realized. Notably, this execution scheduling task is outsourced to the resourceful Server.

To understand the effectiveness of our PAM method to reduce the impact of brownouts so, we execute a computation intensive module, MAC() using PAM, at power-up on a CRFID. We employ a few lines of code to toggle GPIO pins to indicate the successful completion of a routine. Notably, it is difficult to track a device's internal state without a debug tool attached to the device; however, if the debug interface is in use, it will either interfere with powering, or affect the timing by involving additional JTAG service code.

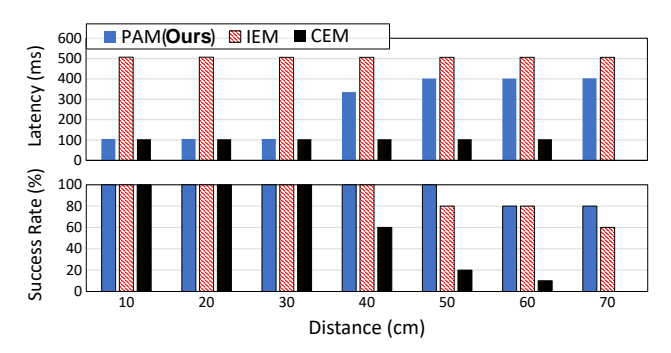


Fig. 7. Experimentally evaluating the latency and success rate of our proposed power aware execution model (PAM) against the IEM method in [13] and a typical continuous execution model (CEM). Notably, CEM fails at 70 cm.

PAM Experimental Validation. We measure the time taken to complete the MAC() execution (latency) and success rate (success over 10 repeated attempts under wireless powering conditions) with digital storage oscilloscope connected to GPIO pins indicating a successful execution before power loss. We compute over a 1,280 Byte message to test the effectiveness of PAM in preventing a power loss event due to brownout and compare performance with the execution method—denoted IEM—of a fixed LPM state (30 ms) *programmatically* encoded during the device provisioning phase as in [13].

The results in Fig. 7 show the effectiveness of PAM to mitigate the interruptions from power loss. This is evident when the success rate results without PAM—using the continuous execution model (CEM)—is compared with those of PAM at increasing operating distances. However, as expected, we

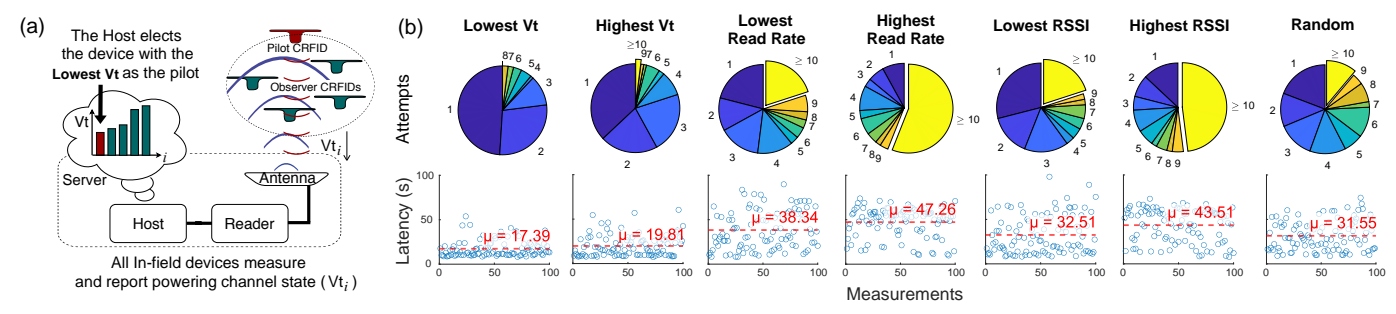


Fig. 8. (a) Our proposed Pilot-Observer method. Only the elected Pilot using the Vt_i based election method responds while *Observers* listen silently. (b) Evaluation of Pilot Token selection strategies. Measured Tokens are placed 40 cm above the reader antenna, where the powering condition is critical. Showing the number of attempts to have all 4 CRFIDs (Tokens) updated (pie chart) and the corresponding latency (scatter plot) over 100 repeated measurements.

can also observe that the dynamically adjusted the execution model parameters ($t_{\rm LPM}$ and $t_{\rm active}$) of PAM at increasing distances to prevent power loss events increase latency or the time to complete the routine. When PAM is compared with IEM, the dynamically adjusted execution model parameters allow PAM to demonstrate an improved capability to manage interruptions from power-loss at increasing distances; this is demonstrated by the higher success rates at distances of 50 cm and 70 cm. Since, IEM encodes operating settings programmatically during the device provisioning phase [13], we can observe increased latency at shorter operating ranges when compare to PAM which allows a completion time similar to that obtained from CEM at shorter distances. Thus, PAM provides a suitable compromise between latency and successful completion of a task at various operating distances.

Pilot-Observer Mode. We observed and also confirmed in Fig. 5 that the task of responding to communication commands will likely cause power loss. During the Secure Broadcast stage shown in Fig. 4, communication is dominated by repeated SecureComm commands with payloads of encrypted firmware and the data flow is uni-directional. Intuitively, we can disable responses from all the tokens to save energy. However, the SecureComm command under EPC Gen2 requires a reply (ACK) from the token to serve as an acknowledgement [30]. An absent ACK within 20 ms will cause a protocol timeout and execution failure.

To address the issue, we propose the pilot-observer mode inspired by the method in Stork [12]. A critical and distinguishing feature of our approach is the intelligent election of a pilot token from all tokens to be updated—we defer to Supp. Material S VI for a more detailed discussion on the differences. As illustrated in Fig. 8(a), our approach places all in-field tokens to be updated into an Observer mode except one token elected by the Server to drive the EPC Gen2 protocol—this device is termed the Pilot token. By doing so, observer tokens process all commands such as SecureComm—ignoring the handle designating the target device for the command—whilst remaining silent or muting replies to all commands whilst in the Observer mode. Muting replies significantly reduce energy consumption and disruption to power harvesting of the tokens.

We propose *electing* the token with the *lowest* reported Vt as the pilot based the following observations: i) measuring powering channel state from the token, obtained from $Vt_i \leftarrow \mathsf{SNIFF}(t)$, is the most reliable measure of power available to a given device (see the discussion in Supp. Material S V);

and ii) allowing the most power starved token to drive the protocol would ensure all other tokens (with higher levels of available power) to successfully process the broadcasted firmware and remain synchronized with the protocol during the update. Hence, if the pilot succeeds, observers are expected to succeed.

Experimental Validation of Pilot Election Method. To demonstrate the effectiveness of our pilot token election method, we considered seven different pilot token selection methods based on token based estimations of available power and indirect methods of estimating the power available to a token by the server: 1) Lowest V_t : this implies the pilot is selected based on the most conservative energy availability at token. 2) Highest V_t : the pilot has to reply to commands, hence we may expect higher power availability to prevent the failure of a broadcast session due to brownout at the pilot; 3) Lowest Read Rate: a slow pilot allows observers to gather more energy during the broadcast and remain synchronized with the protocol to prevent failure of the observer tokens; 4) Highest Read Rate: a faster pilot could reduce latency; 5) Lowest RSSI: successful communication over the poorest channel may ensure all observers are on a better channel (RSSI acts as an indirect measure of the powering channel at the token); 6) Highest RSSI: prevent pilot failure due to a potentially poor powering channel at the pilot token; and 7) Random selection: monkey beats man on stock picks.

We have extensively evaluated and compared all of the above seven pilot token selection methods. The experiment is conducted by placing 4 CRFID tokens at 20 cm, 30 cm, 40 cm and 50 cm above an reader antenna; each CRFID is placed in alignment with the four edges of the antenna (See Fig.10.(d)). We repeated the code dissemination process 100 times at each distance test, for each of the 7 different pilot selection methods. We recorded two measures: i) latency (seconds) as defined in Section V.A; and ii) number of times the broadcast attempt updated all of the 4 in-field devices.

As illustrated in Fig. 8.(b), at 40 cm where the power conditions are more critical at a token, the selected pilot token with the lowest token voltage (Vt) shows an enormous advantage, in terms of both latency and attempt number. Overall, our proposed approach (electing the lowest Vt) ensures that most observer tokens are able to correctly obtain and validate the firmware in a given broadcast session on the first attempt in the critical powering regions of operation (we provide a theoretical justification in Supp. Material S V).

Summary. Our pilot-election based method effectively reduces the chance of power failure as well as desynchronisation of the Observers tokens during a firmware broadcast session. Our approach is able to ensure that more of the Observer devices are able to correctly obtain and validate the firmware during a single broadcast sessions.

C. Efficient Security Primitives

Wisecr requires two cryptogrpahic primitives: i) symmetric key primitive SKP(); and ii) a keyed hash primitive for the message authentication code MAC(). When selecting corresponding primitives in the following, two key factors are necessary to consider:

- Computational cost: The CPU clock cycles required for a primitives quantifies both the computation cost and energy consumption. Therefore, clock cycles required for executing the primitives need to be within energy and computational limitations of the energy harvesting device.
- 2) *Memory needs*: On-chip memory is limited—only 2 KB of SRAM on the target MCU—and must be shared with: i) the RFID protocol implementation; and ii) user code.

Symmetric Key Primitives. We fist compare block ciphers via software implementation benchmarks—clock cycle counts and memory usage—on our target microcontroller [31], [32]. We also considered the increasingly available cryptographic co-processors in microcontrollers: our targeted device uses an MSP430FR5969 microcontroller and embeds an on-chip hardware AES256 engine (we refer to as HW-AES) [33]. Based on the above selection considerations, HW-AES is confirmed to outperform others. Specifically, HW-AES to encrypt/decrypt a 128-bit block consumes 167/214 clock cycles with a power overhead of 21 μ A/MHz; therefore we opted for HW-AES for SKP.Dec function implementation on our target device. Similar hardware AES resources can be found in a variety of microcontrollers, ASIC, FPGA IP core and smart cards. In case of WH-AES is not supported, software AES implementation could be alternative, such as tiny-AES-c.

Message Authentication Code. MACs built upon BLAKE2s-256, BLAKE2s-128, HWAES-GMAC and HWAES-CMAC on our targeted MSP430FR5969 MCU were taken into consideration [13]. We selected the 128-bit *HWAES-CMAC*—Cipherbased Message Authentication Code²—based on AES since it yielded the lowest clock cycles per byte by exploiting the MCU's AES256 (the above HW-AES) engine.

D. Bootloader Control Flow

We can now realize an uninterruptible control flow for an immutable bootloader built upon on the security properties identified and engineered to achieve our *Wisecr* scheme described in Section II-B. We describe the bootleader control flow in Fig. 9.

At power-up, (1) the token performs MCU initialization routines, enables memory protection and carries out a self-test to determine whether the firmware update is required, or

if there is a valid application installed. If no update is required and the user application is valid, the user code is executed 2. Under the application execution mode, the Server $\mathcal S$ may send an Inventory command 3 to instruct the token T to send back e.g., sensed data, 4 or in 5 setup the *FirmwareUpdate* flag and trigger a software reset in preparation for update.

Security Association Upon a software reset, a set *Firmware-Update* flag directs the token T to enter the firmware update mode and 6 reset the *Firmware-Update* flag to ensure a stateless transition to application execution mode in the event of an interrupted update session. 7 Subsequently, the token waits for further instruction from the Server. On reception of an encrypted broadcast session $(\mathbf{sk})_i$ and the MAC tag \mathbf{s}_i of the new firmware, the token T decrypts $(\mathbf{sk})_i$ with its device key \mathbf{k}_i and acquires the session key \mathbf{sk} (\mathbf{s}) .

Secure Broadcast Recall, at this stage, all tokens selected for update will be switched into the observer mode except the pilot token that is set respond to the Server. The pilot token in state (9) receives a new chunk of encrypted firmware (firmware^(j)), and (10) stores it into the specified memory location. In (12), for tokens in observer mode, they solely listen to the communication traffic between the Server and the Pilot token without replying. In other words, tokens under Observer mode receives the encrypted firmware chunks, (13) store chunks in memory but ignores unicast handle identifying the target device; this significantly saves communication energy as detailed in Section III-B2. Once an End of Broadcast (EOB) message is received, all tokens stop waiting for new packets and start firmware decryption (15). In the meantime, tokens reset the ObserverMode flag (14) to return back to normal mode.

Validation: The token computes a local MAC tag \mathbf{s}_i' , including the decrypted firmware, and compares it with the received MAC tag \mathbf{s}_i (16). The firmware is accepted and applied to update (7) the token if \mathbf{s}_i' and \mathbf{s}_i match; otherwise, the firmware is discarded and the update aborted (18). Subsequently, each

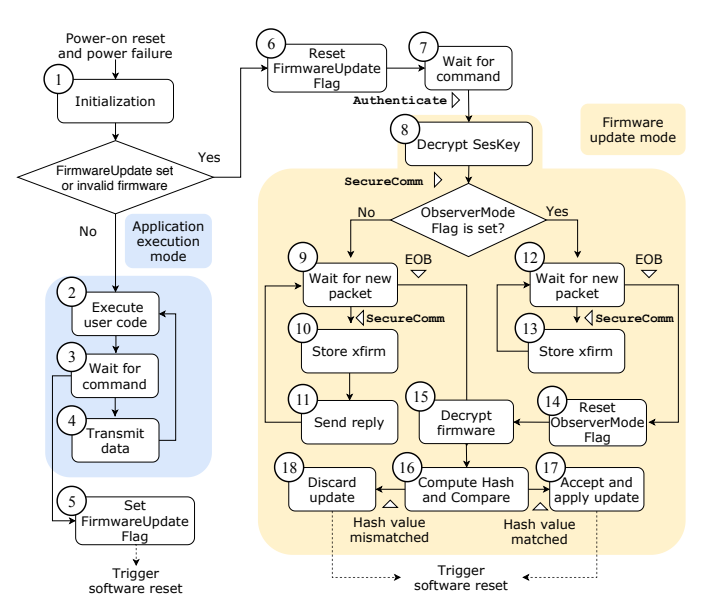
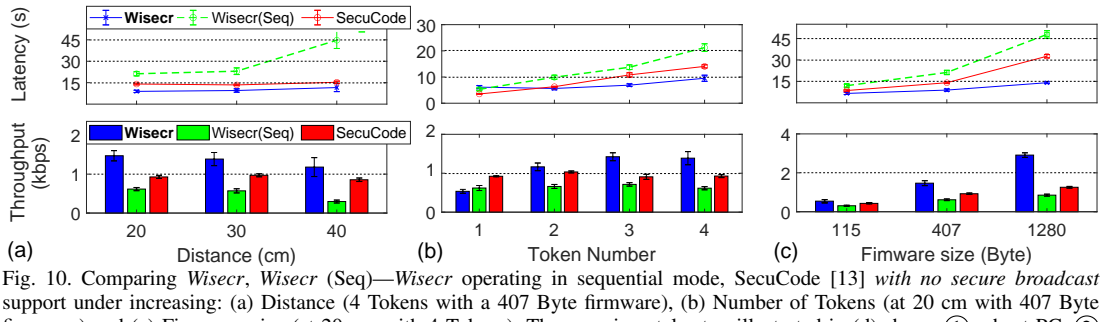
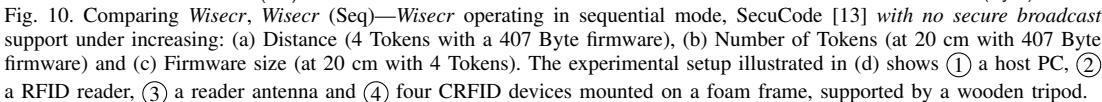
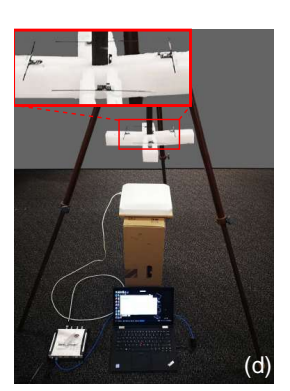


Fig. 9. An overview of the Wisecr Bootloader control flow

²The implementation in NIST Special Publication 800-38B, Recommendation for Block Cipher Modes of Operation: the CMAC Mode for Authentication is used here.







token performs a software reset to execute the new firmware.

Notably, a power-loss event during the control flow will result in a reset and rebooting of the token T and a transition out from the firmware update state. Most significantly, in such an occurrence, the immutable bootloader functionality is preserved. Although the loss of state implies that a Server S must reattempt the secure update, we prevent the token from being left in a vulnerable state to inherently mitigate security threats posed in the power off state [18].

TABLE II. Wisecr Implementation and Execution Overheads

| | Clock Cycles | Memory Usage (Bytes) ROM RAM | | HW Requirement |
|--|--------------|---------------------------------|------------------|------------------|
| Functional blocks | | | | |
| $\mathbf{sk} \leftarrow SKP.Dec_{\mathbf{k}_i}(\langle \mathbf{sk}_i \rangle)$ | 1,106 | 842 ¹ | 62 | HW-AES |
| $firmware^{(j)} \leftarrow SKP.Dec_{sk}(\langle firmware^{(j)} \rangle)$ | 1,106 | 836 | 62 | HW-AES |
| $s_i \leftarrow MAC_{sk}(\mathbf{firmware} \mathbf{ver}_i \mathbf{nver})$ | 17,150 | 2,716 | 58 | HW-AES |
| $Vt_i \leftarrow SNIFF(t)$ | 1,602 | 260 | 10 | ADC |
| PAM.Enter(t_{LPM_i} , t_{active_i}) and PAM.Exit() ² | 81 | 146 | 5 | Timer |
| Stages | | | | |
| Security Association | 2,708 | 1,102 | 72 | ADC, HW-AES |
| Secure Broadcast | 1,187 | 1,096 | 72 | HW-AES, Timer |
| Validation | 17,150 | 2,716 | 58 | HW-AES, Timer |
| Remote Attestation (elaborate mode) | 18,360 | 3,037 | 80 | HW-AES |
| Total | | | | |
| Wisecr (excluding Remote Attestation) | 21,045 | 3,818 ³ | 130 ³ | All of the above |

¹⁶ bytes of this value incorporates the device key \mathbf{k}_i in secure storage

IV. END-TO-END IMPLEMENTATION AND EXPERIMENTS

This section elaborates on software tools, the end-to-end implementaiton of Wisecr and extensive experiments conducted to systematically evaluate the performance of Wisecr.

A. End-to-End Implementation

We implement a bootloader and a Server Toolkit to wirelessly and simultaneously update multiple CRFID transponders using commodity networked RFID hardware and standard protocols. We realize the Wisecr scheme in Fig. 4 and the identified security property requirements. Specifically, we employ MSP430FR5969 MCU based WIPS5.1LRG CRFID devices. The MSP430FR5969 microcontroller has a 2 KB SRAM and a 64 KB FRAM interal memory. The implementation is a significant undertaking and includes software development for the CRFID as well as the RFID reader and backend services for the server update mechanisms. Given that we have open sourced the project, we describe: i) the bootloader in Supp. Material S I; and ii) the Sever Toolkit and the protocols for Host-to-RFID-reader and Reader-to-CRFID-device communications for implementing Wisecr over EPC Gen2 in Supp. Material S II.

B. Wisecr Implementation Overheads

We first evaluate the execution and implementation overhead of each Wisecr security functional block; results are summarized in Table II. The execution overhead is measured in terms of clock cycles for installing a firmware of 240 bytes. The implementation overhead is measured in memory usage, consisting of ROM for code and constants and RAM for runtime state. Secondly, we assess the necessary hardware modules such as hardware AES accelerator (HW-AES), analogto-digital converter (ADC) and Timer. All functional blocks are implemented in platform independent C source files. We summarize the implementation costs for each stage; the most significant implementation and execution overhead is from the Validation stage because of the computationally heavy MAC() function—recall Remote Attestation is an optional stage.

C. Experiment Designs and Evaluations

We employed four WIPS5.1LRG CRFID devices and an Impinj R420 RFID reader with a 9 dBic gain antenna to communicate with and energize the CRFID devices. All of the experiments are conducted with the RFID reader feeding the antenna with 30 dBm output power. Given that, the recent EPC Gen2 V2.0 security commands such as the SecureComm are not yet widely supported by commercial RFID readers, like the Impini Speedway R420, we map the unsupported EPC Gen2 command to the BlockWrite command as in [13]. We summarize our evaluations below³:

• We evaluate performance (latency, throughput) and compare with: i) SecuCode [13]⁴, presently, the only CRFID firmware update scheme considering security—notably, the scheme only prevents malicious code injection attacks but designed to update a single device at a time as shown in the method comparison Table III; ii) Wisecr intentionally set to sequential mode—broadcasting/updating one token at a time—termed Wisecr (Seq), to assess the gains from Wisecr broadcasting firmware to multiple devices simultaneously; and iii) non-secure multi-CRFID dissemination scheme, Stork [12] (see Supp. Material S VII).

³Notably, our extensive experiments to evaluate techniques and modules we developed are detailed in the Appendices with references in the main article

²A single PAM execution, as defined in Fig. 6

⁴In [13], the device key is derived from SRAM PUF responses. In our comparison, we opt for a device key in the protected NVM instead to make a fair overhead comparison. Further, the key derivation module only adds a fixed overhead at start-up.

- We evaluate the efficacy of our Power Aware Execution Model (PAM) and Pilot Token selection method (results in the Section. III-B2).
- We demonstrate *Wisecr* in an end-to-end implementation.

D. Performance Evaluation and Results

We use two performance metrics: i) end-to-end *latency*; and ii) *throughput* (bits per second). Latency is the time elapsed from the Server Toolkit transmitting the firmware to an RFID reader using LLRP commands to the time the Server Toolkit confirms the acknowledgement of successfully updating *all chosen tokens*. Throughput is the total data transferred over the latency, where Throughput (bps) = ($|firmware| \times NoOfTokens$)/ Latency. Our evaluation is carried out under three different controlled variables: i) distance; ii) number of tokens; and iii) firmware size. In each experiment, only one variable is changed and our results are collected over 100 repeated measurements, with outliers outside of 1.5 times upper and lower quartiles removed.

First, we transfer the same firmware code (a 407 Byte accelerometer service) to four target devices located at distances from 20 cm to 40 cm, covering good to poor powering channel states, to evaluate the *stability* of the *Wisecr* scheme. As expected, we can observe in Fig. 10(a) that the performance of all three schemes downgrades with increasing distance.

Notably, Wisecr and SecuCode outperforms the Wisecr (Seq). Because, Wisecr (Seq) incurs a larger overhead through the need for executing a Security Association stage to setup the broadcast security parameters, for each device. Further, SecuCode (without IP protection) does not need to execute the power intensive firmware decryption operations, and thus is less likely to encounter power-loss and update session failure or require the extra time necessary by Wisecr to decrypt the firmware. As expected, Wisecr outperforms albeit the added security functions provided in comparison to SecuCode.

Second, following the method and metrics in Stork [12], we tested the performance of the schemes by increasing the number of CRFID devices to be updated. We can see in Fig. 10(b) that the latency of both *Wisecr* (Seq) and SecuCode increases linearly while *Wisecr* remains relatively steady regardless of the number of devices to update. Consequently, *Wisecr* exhibits significantly improved throughput as the number of device increases. Further, we examine performance under increasing firmware size: 115 Bytes; 407 Bytes (a sensor service code); and 1280 Bytes (a computation code firmware). Efficacy of broadcasting to multiple devices simultaneously is validated by latency and throughput performance detailed in Fig. 10(c).

Third, all three candidates show improved efficiency as larger firmware sizes are transmitted; *Wisecr*'s significantly better efficiency can be attributed to the broadcast method.

End-to-End Demonstration. A demonstration of the firmware update process in an end-to-end implementation is available at https://youtu.be/'OuStZsTyV8. In 100 repeated updates, Wisecr successfully broadcast to all devices in the first attempt in 81% of the time. We open source the complete source code for Wisecr and related tools at https://github.com/AdelaideAuto-IDLab/Wisecr.

E. Security Analysis

Under the threat model in Section II-A, we analyze *Wisecr* security against: i) IP theft (code reverse engineering); ii) malicious code injection attacks under code alteration, loading unauthorized code, loading code onto an unauthorized device, and code downgrading; and iii) incomplete code installation.

IP Theft or Code Reverse Engineering. The wirelessly broadcasted firmware is encrypted using a one-time 128-bit broadcast session key \mathbf{sk}_i . Without the knowledge of the broadcast session key, the adversary \mathcal{A} is unable to obtain the plaintext **firmware** through passive eavesdropping. Once the firmware is decrypted on the token, the binaries cannot be accessed outside the immutable bootloader. Therefore, the probability of a successful IP theft is now determined by the security provided by the size of the selected keys. Hence, the probability of the adversary \mathcal{A} obtaining the **firmware** is no more than the brute-force attack probability 2^{-128} .

Loading Unauthorized Code. The security property of a MAC tag $\mathbf{s}_i \leftarrow \mathsf{MAC}_{\mathbf{k}_i}(\mathbf{firmware}||\mathbf{ver}_i||\mathbf{nver})$ ensures that the adversary A cannot commit a malicious firmware injection attack without the knowledge of the session key sk and/or device key \mathbf{k}_i —recall that the sharing of $\mathbf{s}\mathbf{k}$ is protected through a secure channel established with the token specific private key \mathbf{k}_i . Specifically, only the Server with the $\mathbf{s}\mathbf{k}$ is able to produce a valid MAC tag to a token T. Hence, the probability of launching a successful attack by the adversary A is limited to the probability of successfully guessing the device key \mathbf{k}_i and/or guessing the session key $\mathbf{s}\mathbf{k}$ in a manin-the-middle attack to successfully construct a MAC tag and disseminate a malicious firmware that will be correctly validated by the target tokens. Therefore, without knowledge of \mathbf{k}_i or \mathbf{sk} , the probability of fooling a token T to inject a malicious firmware by A is no more than the brute-force attack probability 2^{-128} determined by the key size $|\mathbf{k}_i| = 128$.

Code Alteration. For each firmware update, a MAC tag $\mathbf{s}_i \leftarrow \mathsf{MAC}_{\mathbf{k}_i}(\mathsf{firmware}||\mathbf{ver}_i||\mathbf{nver})$ is used to verify code integrity. Therefore, without knowledge of the session key \mathbf{sk} , the adversary \mathcal{A} can not generate a valid MAC tag for an altered firmware. Any attempted changes to the firmware during the code dissemination will be detected and, thus, firmware discarded by the token. Further, the attacker \mathcal{A} cannot generate a valid MAC tag for a crafted firmware \mathcal{A} without successfully fooling the tag to accept the crafted session key $\mathbf{sk}_i^{\mathcal{A}}$; as before, the probability of the attacker's success is 2^{-128} when $|\mathbf{k}_i| = 128$ (recall that the session key \mathbf{sk} is shared through a secure channel established with device key \mathbf{k}_i that is unknown to the adversary).

Loading Code onto an Unauthorized Device. Each authorized device i maintains a unique and secret device specific key \mathbf{k}_i only known to the Server \mathcal{S} . Therefore, an unauthorized device cannot decrypt the session key $\mathbf{s}\mathbf{k}_i$ to install a recorded firmware encrypted with $\mathbf{s}\mathbf{k}_i$ of an authorized device.

Code Downgrading. The adversary \mathcal{A} can attempt to downgrade the firmware to an older version to facilitate subsequent exploitation of potential vulnerabilities in a previous distribution. This can be attempted through a replay attack by

impersonating the Server. However, for each firmware update, a specific MAC tag: $\mathbf{s}_i \leftarrow \mathsf{MAC}_{\mathbf{k}_i}(\mathsf{firmware}||\mathbf{ver}_i||\mathbf{nver})$ is generated based on two monotonically increasing version numbers: \mathbf{ver}_i and \mathbf{nver} . Without direct access to modify the Secure storage contents in region M to re-write the current version number of a device to an older version, the attacker cannot replay a recorded MAC tag from a previous session to force a token to accept an older firmware. By virtue of the monotonically increasing version numbers, and the secure MAC primitive protected by the session key \mathbf{sk} , a successful software downgrade using a replay attack cannot be mounted by the adversary \mathcal{A} .

Incomplete Firmware Installation. The adversary A may attempt to prevent a new firmware installation and spoof a device response with an updated version number during an interrogation—the version number is public information and sent in plaintext as shown in Fig. 4. Hence, a token may be left executing an older firmware version with potential firmware vulnerabilities. The Server can verify that a specific disseminated firmware deployed by the token is the same as the one issued by the Server by performing a remote attestation. In our Wisecr scheme, we have considered an optional remote attestation stage (detailed in Section II-B and the Supp. Material S III) to allow the Server to verify the firmware installation on a given token. In general, both code installation attestation is bounded to the device key k_i , thus, it is infeasible to fool the Server without knowledge of the device key.

V. RELATED WORK AND DISCUSSION

Here, we discuss related works in the area of wireless code dissemination to CRFID devices. Notably, the topic of wireless code updating has been intensively studied for battery powered Wireless Sensor Network (WSN) nodes. For example, a recent study by Florian et al. [24] proposed updating the firmware and peer-to-peer attestation of multiple mesh networked IoT devices. Physical unclonable functions [13] and blockchains [34] have also been utilized in code dissemination But, such schemes [24], [34] are designed for battery powered WSN nodes featuring device-to-device communication capability, and supervisory control of operating systems (e.g. TinyOS), absent in batteryless CRFID devices (see challenges C1 to C4 in Section I). Further, batteryless devices operate under extreme energy and computational capability limitations. In particular, harvested energy is intermittent and limited and thus devices face difficulties supporting security functions such as key exchange using Elliptic Curve Diffie-Hellman used in [24]. Therefore, we focus on research into wireless dissemination schemes for CRFID like devices in our discussions. Further, we also discuss and compare our work with existing wireless methods developed for CRFID to highlight the aim of our scheme to fulfil unmet security objectives for simultaneous wireless firmware update to multiple CRFIDs.

Wireless Code Dissemination to CRFID. Given the recent emergence of the technology, there exists only a few studies on code dissemination to CRFID devices. Wisent from Tan $et\ al.\ [14]$, and R^3 from Wu $et\ al.\ [17]$ demonstrate a

wireless firmware update method for CRFIDs. Subsequently, Aantjes et al. [12] proposed Stork, a fast multi-CRFID wireless firmware transfer protocol. Stork forces devices to ignore the RN16 handle in down-link packets—a form of promiscuous listening-to realize a logical broadcast channel in the absence of EPC Gen2 support for a broadcast capability; RN16 specifies the designated packet receiver. This technique enables Stork to simultaneously program multiple CRFIDs to achieve fast firmware dissemination. Our pilot-Observer mode (Section III-B2) is based on a similar concept, but instead of always selecting the first seen device, as in Stork, we strategically elect the token with the lowest V_t as the Pilot to achieve higher broadcast success. Brown and Pier from Texas Instrument (TI) developed MSPBoot [35] in late 2016. They demonstrate an update using a UART or SPI bus to interconnect a MSP430 16-bit RISC microcontroller and a CC1101 sub-1GHz RF transceiver.

However, none of the schemes, *Wisent*, R^3 , Stork and the work in [35], considers security when wirelessly updating firmware. SecuCode [13] recently took the first step to prevent malicious code injection attacks where a single CRFID device is updated in turn. But SecuCode is lacks scalability and performs device by device updates, cannot protect the firmware IP, and provides no validation of firmware installation.

Remote Attestation. Attestation enables the Server to establish trust with the token's hardware and software configuration. Existing mainstream remote attestation methods are unsuitable for a practicable realisation in the context of intermittently powered, energy harvesting platforms we focus on. For example, peer-to-peer attestation adopted in [24] is impractical in the CRFID context due to the lack of a device-to-device communication channel. In boot attestation [36], a public-key based scheme is proposed to fit ownerhsip and third party attestation, however public-key schemes are too computationally intensive for the batteryless devices we consider. Recently, a publish/subscribe mechanism based asynchronous attestation for large scale WSN is presented in SARA [37], however, such a publish/subscribe paradigm is yet to be supported over a standard EPC Gen2 protocol. In contrast, our lightweightremote-attestation mechanisms (see Section II-B) are inspired from the recent study in [15] where methods are designed for resource limited platforms and require no additional building blocks besides those necessary for Wisecr.

TABLE III. Comparison with Related Studies.

| Work | | Power-loss mitigation | | Security | | | Dublic |
|---------------------|---------------------|--------------------------------|-----------------|---|------------------------|----------------------|-------------------------------------|
| | Multiple devices | Commun. Energy Reduction | Adaptive IEM | Prevent Malicious Code Injection | Prevent IP Theft | Code instal. attest. | Public source code release |
| Wisent [14] | × | × | × | × | × | × | / |
| R ³ [17] | × | × | × | × | × | × | × |
| Stork [12] | ✓ | / | × | × | × | × | 1 |
| SecuCode [13] | × | × | × | / | × | × | 1 |
| Wisecr (Ours) | / | / | / | / | / | / | / |

Comparisons. A comparison of *Wisecr* with wireless code dissemination studies *specific to passive CRFID devices* is summarised in Table III. *Wisecr* is the only *secure* scheme (prevent IP theft and malicious code injection, and provide attestation of firmware installation) for *simultaneous* update of

passively powered devices. We have also extensively compared the performance of *Wisecr* with the *non-secure* code update method of *Stork* to provide an appreciation for the security overhead in an end-to-end implementation in **Supp. Material S VII**.

VI. CONCLUSION

Our study proposed and implemented the first secure and simultaneous wireless firmware update to many RF-powered devices with remote attestation of code installation. We explored highly limited resources and innovated to resolve security engineering challenges to implement *Wisecr*. The scheme prevents malicious code injection, IP theft, and incomplete code installation threats whilst being compliant with standard hardware and protocols. *Wisecr* performance and comparisons with state-of-the-art through an extensive experiment regime have validated the efficacy and practicality of the design, whilst the end-to-end implementation source code is released to facilitate further improvements by practitioners and the academic community.

REFERENCES

- B. Lucia, V. Balaji, A. Colin, K. Maeng, and E. Ruppel, "Intermittent computing: Challenges and opportunities," in *Summit on Advances in Programming Languages*, 2017.
- [2] A. P. Sample, D. J. Yeager, P. S. Powledge, A. V. Mamishev, and J. R. Smith, "Design of an RFID-based battery-free programmable sensing platform," *IEEE Trans. Instrum. Meas.*, vol. 57, no. 11, pp. 2608–2615, 2008.
- [3] H. Zhang, J. Gummeson, B. Ransford, and K. Fu, "Moo: A batteryless computational RFID and sensing platform," *Uni. of Massachusetts* Comput. Sci. Technol. Report UM-CS-2011-020, 2011.
- [4] Farsens, "Pyros-0373 UHF RFID battery-free temperature sensor tag," http://www.farsens.com/en/products/pyros-0373/, accessed: 2020-07-28.
- [5] A. J. Bandodkar, P. Gutruf, J. Choi, K. Lee, Y. Sekine, J. T. Reeder, W. J. Jeang, A. J. Aranyosi, S. P. Lee, J. B. Model *et al.*, "Battery-free, skin-interfaced microfluidic/electronic systems for simultaneous electrochemical, colorimetric, and volumetric analysis of sweat," *Science Advances*, vol. 5, no. 1, p. eaav3294, 2019.
- [6] R. L. Shinmoto Torres, R. Visvanathan, D. Abbott, K. D. Hill, and D. C. Ranasinghe, "A battery-less and wireless wearable sensor system for identifying bed and chair exits in a pilot trial in hospitalized older people," *PLOS ONE*, vol. 12, no. 10, pp. 1–25, 2017.
- [7] W. Li, H. Song, and F. Zeng, "Policy-based secure and trustworthy sensing for internet of things in smart cities," *Internet of Things J.*, vol. 5, no. 2, pp. 716–723, 2017.
- [8] M. Noura, M. Atiquzzaman, and M. Gaedke, "Interoperability in internet of things: Taxonomies and open challenges," *Mobile Net. and App.*, vol. 24, no. 3, pp. 796–809, 2019.
- [9] A. Parks, "WISP 5," https://github.com/wisp/wisp5, 2016.
- [10] Z. Ning and F. Zhang, "Understanding the security of arm debugging features," in *Proc. IEEE Symp. on Secur. and Privacy (S&P)*, 2019, pp. 602–619.
- [11] F. Xu, W. Diao, Z. Li, J. Chen, and K. Zhang, "Badbluetooth: Breaking android security mechanisms via malicious bluetooth peripherals." in Proc. Network and Distributed Syst. Secur. Symp. (NDSS), 2019.
- [12] H. Aantjes, A. Y. Majid, P. Pawełczak, J. Tan, A. Parks, and J. R. Smith, "Fast Downstream to Many (Computational) RFIDs," in *Proc. IEEE Int. Conf. on Comput. Commun. (INFOCOM)*, 2017.
- [13] Y. Su, Y. Gao, M. Chesser, O. Kavehei, A. Sample, and D. Ranasinghe, "Secucode: Intrinsic PUF entangled secure wireless code dissemination for computational RFID devices," *IEEE Trans. on Dependable and Secur. Comput.*, vol. Early Access, 10.1109/TDSC.2019.2934438, 2019.
- [14] J. Tan, P. Pawelczak, A. Parks, and J. R. Smith, "Wisent: Robust downstream communication and storage for computational RFIDs," in *Proc. IEEE Int. Conf. on Comput. Commun. (INFOCOM)*, 2016, pp. 1–9.
- [15] D. Dinu, A. S. Khrishnan, and P. Schaumont, "SIA: Secure intermittent architecture for off-the-shelf resource-constrained microcontrollers," in IEEE Int. Symp. on Hardware Oriented Secur. and Trust (HOST), 2019, pp. 208–217.

- [16] K. Maeng, A. Colin, and B. Lucia, "Alpaca: intermittent execution without checkpoints," *Proc. of the ACM on Programming Languages*, vol. 1, no. OOPSLA, p. 96, 2017.
- [17] D. Wu, L. Lu, M. J. Hussain, S. Li, M. Li, and F. Zhang, "R3: Reliable over-the-air reprogramming on computational RFIDs," ACM Trans. on Embedded Comput. Syst., vol. 17, no. 1, p. 9, 2018.
- [18] A. S. Krishnan and P. Schaumont, "Exploiting security vulnerabilities in intermittent computing," in *Int. Conf. on Secur., Privacy, and Applied Cryptography Eng. (SPACE)*, 2018, pp. 104–124.
- [19] Z. Liu, H. Seo, Z. Hu, X. Hunag, and J. Großschädl, "Efficient implementation of ECDH key exchange for MSP430-based wireless sensor networks," in *Proc. ACM Symp. on Inf., Comput. and Commun. Secur. (CCS)*, 2015, pp. 145–153.
- [20] Z. Liu, H. Seo, S. S. Roy, J. Großschädl, H. Kim, and I. Verbauwhede, "Efficient ring-LWE encryption on 8-bit AVR processors," in *Int. Work-shop on Crypto. Hardw. and Embed. Syst. (CHES)*, 2015, pp. 663–682.
- [21] F. Brasser, D. Gens, P. Jauernig, A.-R. Sadeghi, and E. Stapf, "Sanctuary: Arming trustzone with user-space enclaves." in *Proc. Network and Distributed Syst. Secur. Symp. (NDSS)*, 2019.
- [22] T. Frassetto, P. Jauernig, C. Liebchen, and A.-R. Sadeghi, "IMIX: In-process memory isolation extension," in *Proc. 27th USENIX Secur. Symp. (USENIX Security)*, 2018, pp. 83–97.
- [23] C. Jin and M. van Dijk, "Secure and Efficient Initialization and Authentication Protocols for SHIELD," *IEEE Trans. Depend. Secur. Comput.*, 2017.
- [24] F. Kohnhäuser and S. Katzenbeisser, "Secure Code Updates for Mesh Networked Commodity Low-End Embedded Devices," in *Proc. Springer Eur. Symp. on Res. in Comput. Secur. (ESORICS)*, 2016, pp. 320–338.
- [25] W. Feng, Y. Qin, S. Zhao, Z. Liu, X. Chu, and D. Feng, "Secure code updates for smart embedded devices based on PUFs," in *Proc. Int. Conf.* on Crypto. and Net. Secur. (CANS), 2017, pp. 325–346.
- [26] F. Piessens and I. Verbauwhede, "Software security: Vulnerabilities and countermeasures for two attacker models," in *Proc. Conf. on Design*, *Automation & Test in Europe (DATE)*, 2016, pp. 990–999.
- [27] A. Aysu, E. Gulcan, D. Moriyama, P. Schaumont, and M. Yung, "End-to-end design of a PUF-based privacy preserving authentication protocol," in *Proc. Springer Int. Workshop on Crypto. Hardw. and Embed. Syst* (CHES), 2015, pp. 556–576.
- [28] P. Thanigai and W. Goh, "Msp430 fram quality and reliability," Texas Instruments, SLAA526A, 2014.
- [29] M. Buettner, B. Greenstein, and D. Wetherall, "Dewdrop: an energy-aware runtime for computational RFID," in *Proc. USENIX Symp. on Net. Syst. Design and Impl. (USENIX NSDI)*, 2011, pp. 197–210.
- [30] G. EPCglobal, "Inc.,"EPCTM Radio-Frequency Identity Protocols Class-1 Generation-2 UHF RFID Protocol for Communications at 860MHz-960MHz Version 2.0.1," EPCGlobal Inc., Technal. Rep., April 2015., Tech. Rep., 2015.
- [31] B. Buhrow, P. Riemer, M. Shea, B. Gilbert, and E. Daniel, "Block cipher speed and energy efficiency records on the MSP430: System design trade-offs for 16-bit embedded applications," in *Int. Conf. on Crypto.* and Inf. Secur. in Latin America (LATINCRYPT), 2014.
- [32] D. Dinu, Y. Le Corre, D. Khovratovich, L. Perrin, J. Großschädl, and A. Biryukov, "Triathlon of lightweight block ciphers for the internet of things," *J. of Crypto. Eng.*, vol. 9, no. 3, pp. 283–302, 2019.
- [33] T. Instruments, "MSP430FR58xx, MSP430FR59xx, MSP430FR68xx, and MSP430FR69xx Family User's Guide," *Texas Instruments*, 2014.
- [34] B. Lee and J.-H. Lee, "Blockchain-based secure firmware update for embedded devices in an internet of things environment," *The Journal of Supercomputing*, vol. 73, no. 3, pp. 1152–1167, 2017.
- [35] L. Reynoso, "Mspboot Main Memory Bootloader for MSP430 ™ Microcontrollers," jun 2013. [Online]. Available: http://www.ti.com/lit/an/slaa600d/slaa600d.pdf
- [36] S. Schulz, A. Schaller, and et al., "Boot attestation: Secure remote reporting with off-the-shelf IoT sensors," in Proc. Eur. Symp. on Res. in Comput. Secur. (ESORICS), 2017, pp. 437–455.
- [37] E. Dushku, M. M. Rabbani, M. Conti, L. V. Mancini, and S. Ranise, "SARA: Secure asynchronous remote attestation for IoT systems," *IEEE Trans. on Info. Forensics and Secur.*, 2020.
- [38] D. E. Holcomb, W. P. Burleson, and K. Fu, "Power-up SRAM state as an identifying fingerprint and source of true random numbers," *IEEE Trans. on Comput.*, vol. 58, no. 9, pp. 1198–1210, 2008.
- [39] R. Maes, A. Van Herrewege, and I. Verbauwhede, "PUFKY: A fully functional PUF-based cryptographic key generator," in *Int. Workshop* on Crypto. Hardw. and Embed. Syst. (CHES), 2012, pp. 302–319.
- [40] P. V. Nikitin, R. Martinez, S. Ramamurthy, H. Leland, G. Spiess, and K. Rao, "Phase based spatial identification of UHF RFID tags," in *Int. Conf. on RFID (IEEE RFID)*, 2010, pp. 102–109.

Supplementary Materials for Wisecr

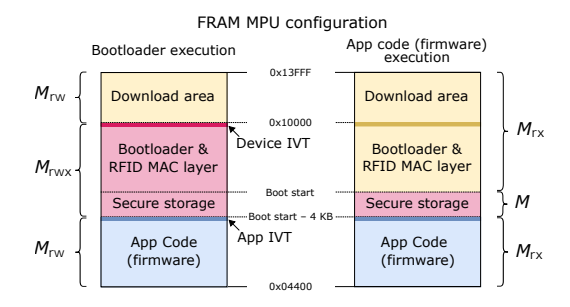


Fig. S1. Memory Protection Unit (MPU) segmentation diagram and memory arrangement during bootloader execution (left) and application code execution (right). Due to hardware limitations, only 3 segments can be defined, and the secure storage area must be at least 4 KB in size due to segment boundary alignment requirements⁶

S I. BOOTLOADER AND MEMORY MANAGEMENT

Wisecr Bootloader. The immutable bootloader supervises firmware execution while needing to be compatible with standard protocols, we developed our bootloader based on the Texas Instrument's recent framework for wireless firmware updates—MSP430FRBoot⁵—and the code base from recent work [13] employing the framework. Such construction ensures a standard tool chain for compilation and update of new firmware whilst the usage of industry standards is likely to increase adoption in the future. We compile the firmware code into ELF (Executable and Linkable Format) made up of binary machine code and linker map specifying the target memory allocation—the memory arrangement is illustrated Fig. S1 and detailed in the Supp. Material S I.

Wisecr Memory Management. For implementing the Secure Storage component, several different mechanisms can be used:

- 1) **Isolated segments (e.g. using IP encapsulation hardware).** *Requirements and limitations*: It requires hardware features (such as IP encapsulation) to implement.
- 2) Execute only memory (e.g. using MPU segments at compile time) In this scheme secure memory is encoded as instructions (e.g. MOV) in execute only memory (XOM) (see [24]). Requirements and limitations: Implementation can be complex, since any code in this region must ensure that it does not leak data (e.g. in CPU registers or volatile memory), including from arbitrary jumps into the code. Additionally, since the bootloader is also unable to write to this region, it cannot be used to protect dynamic secrets (e.g. the broadcast session key).
- 3) Runtime access protection (e.g. using MPU segments at runtime) In this scheme, secure storage is available on device boot-up, but is locked (until next boot-up) by the bootloader before any application code is executed. We employed this method and the implemented memory arrangement is described in Fig.S1. Switching to privilege

mode is done by the bootloader on boot up, and the applications do not need to make any specific modifications. If an application attempts to access a privileged resource, e.g. overwriting the bootloader segment, a power-up clear (PUC) will be triggered by the MPU to cause reboot, before any risky operation. *Requirements and limitations*: Method requires MPU hardware with runtime configuration and locking, and the implementation must ensure that the MPU is always configured correctly before any application code is executed.

4) Volatile secret keys (see, for example, SRAM PUF [38], [39]). Requirements and limitations: It might be computationally expensive to derive and erase the secret key, need a mechanism to 'restore' the volatile area on device restart, and a different mechanism is required to ensure the bootloader is immutable.

S II. DETAILED Wisecr UPDATE SCHEME

Server Toolkit. Our Server Toolkit can be executed on a host with network connectivity to an RFID reader. The App loads in the ELF file generated from the compilation process, parses and slices it into MSPBoot specified 128-bit-long commands suitable for the RFID reader. The App then uses LLRP commands to construct AccessSpecs and ROSpecs. These encode *EPC C1Gen2* protocol commands such as BlockWrite and SecureComm commands to discover, engage and configure a networked RFID reader to execute the *Wisecr* protocol. Notably, we follow the same protocols for Host-to-RFID-reader and Reader-to-CRFID-device communications as in [12], [13] and detail implementation of *Wisecr* over *EPC Gen2* in the Fig. 3.

Wisecr Update Scheme Over EPC Gen2. As described in Fig.4, Wisecr enables the ability to distribute and update firmware of multiple CRFID tokens, simultaneously. Given that a Server S communicates with an RFID device using EPC Gen2, a practicable, scalable and secure code dissemination scheme must be implemented over EPC Gen2. This requires communication between three separate entities: i) the host machine; ii) the reader; and iii) CRFID transponders—see main text Fig. 3. Our scheme description here focuses on the communication between CRFID devices—tokens T—and the RFID reader—the Server S over the EPC Gen2 protocol as illustrated in Fig. S2—our open source code base provides a complete description (https://github.com/AdelaideAuto-IDLab/Wisecr).

S III. REMOTE ATTESTATION

We develop two attestation modes, the *fast* mode and the *elaborate* mode considering the power and computation limitations. In the *fast* mode, we sacrifice the veracity of the attestation by only exagmining the token serial number (**id**) and the version number (**ver**_i). In addition, different from the *fast* mode, the *elaborate* mode traverses over an entire memory segment. The *elaborate* mode is relatively more time

⁵R, Brown et.al. (Mar, 2020) MSP430FRBoot – "Main Memory Bootloader and Over-the-Air Updates for MSP430TM FRAM Large Memory Model" Available: https://www.ti.com/lit/an/slaa721e/slaa721e.pdf (20 Jan 2021)

⁶W, Goh et.al. (Jun, 2020) "MSP430 FRAM Technology" Available: https://www.ti.com/lit/an/slaa628a/slaa628a.pdf (20 Jan 2021)

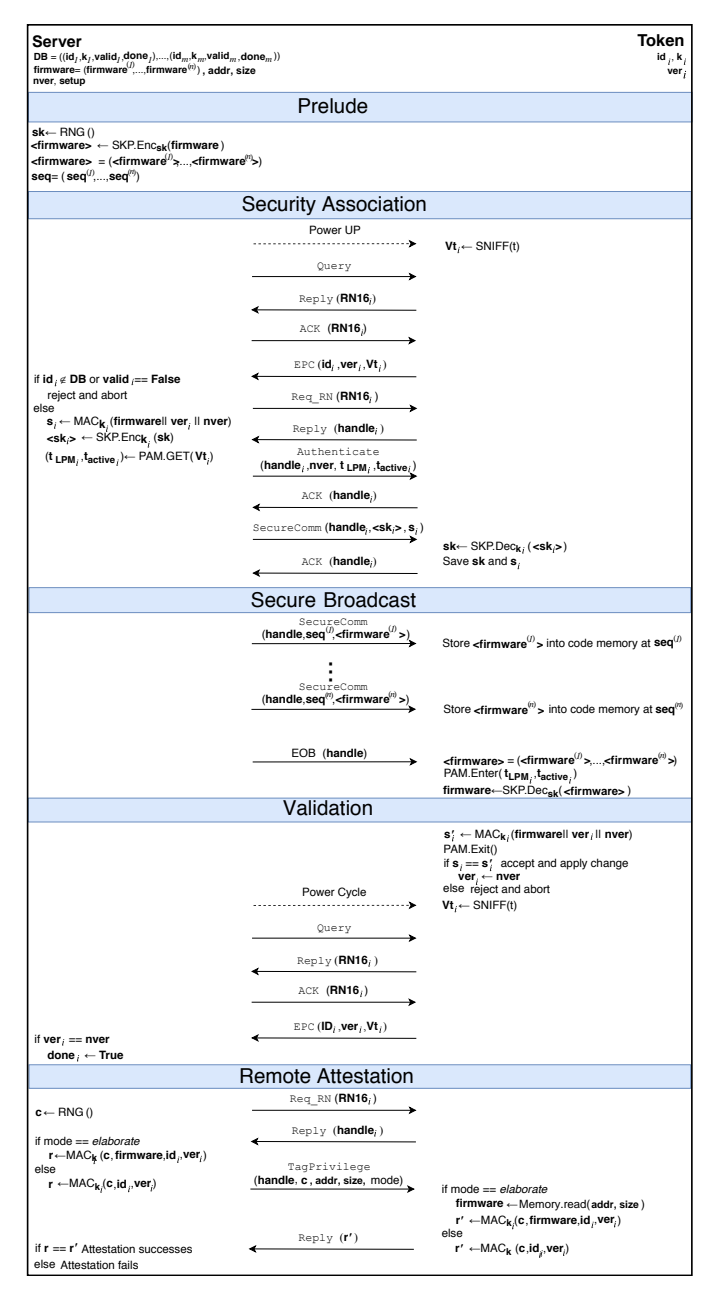


Fig. S2. Wisecr protocol implemented over the EPC Gen2 protocol.

consuming but allows the further security provision to directly verify the code installed on the target token T_i .

As shown in Fig.S3 (a) Remote Attestation routine is an integral part of the immutable bootloader, it has access to all memory segments: Token device key \mathbf{k} , version number \mathbf{ver}_i , tag serial number \mathbf{id} and the installed user application code **firmware**. A **challenge** is a one-time use random string that is generated by the Server \mathcal{S} . The **response** is the report to be transferred back to the Server. In the *fast* mode illustrated in Fig.S3 (b), the **response** is calculated based on \mathbf{id} and \mathbf{ver}_i . In contrast, the **response** is computed over an entire memory segment, such as the **firmware**, in the *elaborate* mode as depicted in Fig.S3 (c). Remote Attestation is initiated by a standard *EPC Gen2* TagPrivilege command as described in Fig.4.

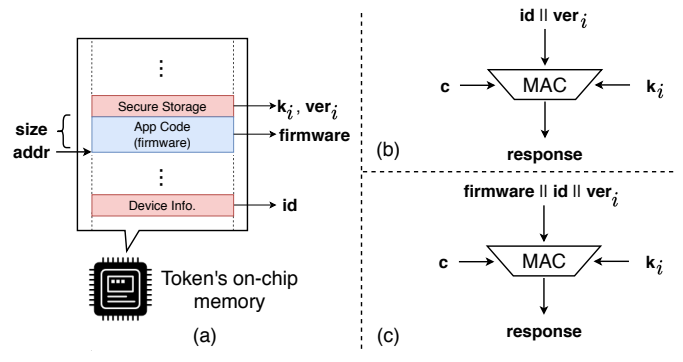


Fig. S3. (a) Token memory and allocations, (b) fast mode, (c) elaborate mode.

S IV. LOW OVERHEAD EXECUTION SCHEDULING

Buettner, *et al.* proposed Dewdrop [29] execution model to *prevent* a brownout event under unreliable powering by executing tasks only when they are likely to succeed by monitoring the available harvested power. Dewdrop explores a dynamic on-device task scheduling method, however, requires the overhead of collecting samples of the harvester voltage and task scheduling by the device's application code.

In addition, Dewdrop is only suitable for CRFID devices equipped with a passive charge pump, such as WISP4.1 [2] since Dewdrop requires directly measuring the charging rate of the reservoir capacitor—charge storage element. In the follow-up, WISP version 5.1, the passive charge pump is replaced with a S-882z active charge pump and the reservoir capacitor is only connected to the load when $V_{\rm cap}$ developed across the capacitor exceeds the reference voltage of 2.4 V ($V_{\rm ref}$). Consequently, in WISP 5.1 the voltage delivered to the microcontroller is a sharp step-up, rather than a ramp-up function related to harvested power. Therefore, the charging-up process cannot be directly monitored by the technique in Dewdrop.

S V. POWERING CHANNEL STATE MEASUREMENT AND POWER AWARE EXECUTION MODEL (PAM)

Observation. Generally, increasing distance of the token from a powering source lowers the harvester output power, RSSI and Read Rate of a given token.

Proposition. Measure powering channel state from the token is the most reliable measure of power available at a device.

Validation.

$$RSSI = P_t G_t^2 G_{path}^2 K$$
 where $G_{path} = \left(\frac{\lambda}{4\pi d_o}\right)^2 |H|^2$ (1)

$$H = 1 + \sum_{i=1}^{N} g_t^i g^i \Gamma_i \frac{d_o}{d_i} e^{-jk(d_i - d_e)}$$
 (2)

Although RSSI or received message rate (Read Rate) [14] measured by an RFID reader (Server) could provide a simple method to measure the powering channel state at a CR-FID transponder, we observed these measures to be highly unreliable. This can be mostly understood by considering the complexity of the signal propagation model [40]—see equations (1) to (2) for details. We can see that RSSI depends

not only on the transmit power P_t , the transmitter antenna gain G_t and backscatter coefficient K, but also the path gain G_{path} . However, G_{path} depends on signal wavelength λ , line of sight distance d_0 and the multi-path factor H; whre, H is a complex function of angle alignment of the transmitter g_t^i and the device g^i , angle-dependent reflection coefficient Γ_i of i-th object, i-th path length for a total of N multi-paths—and the influences from the random access nature i0 of the media access control protocol used by the RFID air interface affecting RSSI and read rate measurements.

Therefore, the powering channel state is best estimated by the field deployed CRFID device harvesting available power at the device.

Thus, we introduce a power aware execution model where:

- The powering channel state at a CRFID tag is measured by the device using a single measurement of harvested power at boot-up (called a *Power Sniff* denoted as $Vt_i \leftarrow SNIFF(t)$ in the update scheme). The voltage measure, Vt_i , is used to estimate the power that can be harvested by a given CRFID device in the field; and
- The workload of scheduling execution of on-device tasks is determined by the resourceful Server (RFID reader and network infrastructure) as opposed to the resource limited CRFID device based on the channel state measurements from a CRFID.

We consider a harvesting device operating under the commonly used charge-burst mode where charge is first accumulated in a storage element—often a capacitor—and charge is released for useful work when an adequate mount of charge (measured in terms of the voltage) is reached at the charge storage element. Our power aware execution model (PAM) requires the Server (RFID reader and/or host) involved in the update to derive two parameters: i) time estimation to charge to a set voltage (t_c) ; ii) time estimation to a brown-out (t_b) based on the CRFID reported measurement \mathbf{Vt}_i . Here, we reason that the distance between the antenna and the given CRFID device does not change during a given update session. Therefore, the power estimated at the begining of the session is valid during the entire session.

Unfortunately, the RF energy harvester on a CRFID device is a non-linear circuit component whose output voltage changes over time as input RF power level varies. Therefore, it is non-trivial to model the RF energy harvester [29]. ETherefore, instead of relying on an analytical model, we adopt an experimental method to derive the parameters for PAM empirically. We measure, in repeated measurements, the output voltage generated by the power-harvesting network on the WISP CRFID. We also measure the expected workload we can obtain from a CRFID device, before a brownout causes power loss. We extrapolate from these measurements to construct an empirical model for the PAM() function employed by the Server to determine the best set of execution parameters from the reported voltage Vt at runtime.

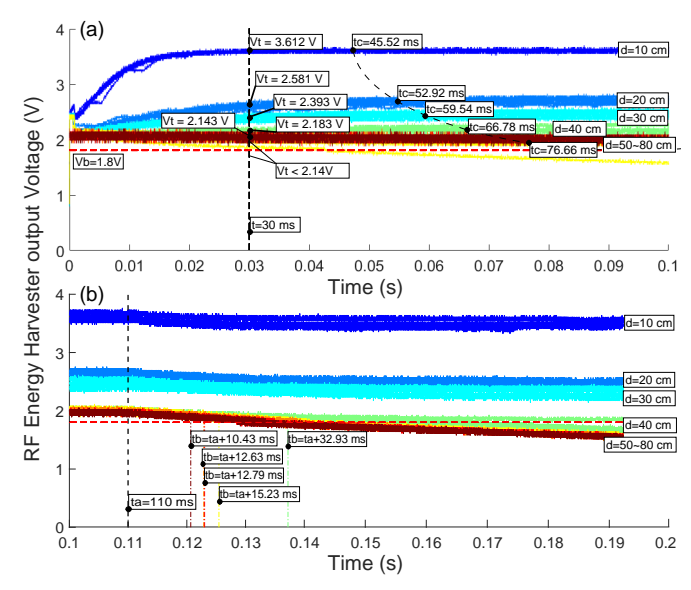


Fig. S4. Power measurements. (a) Charging while the MCU is in LPM mode and (b) discharging when the MCU is in active mode (we employed a MAC computation for the task). The charge and discharge experiments at each fixed distance were repeated 10 times to obtain a mean response.

As depicted in Fig.S4 (a), the output voltage from the charge pump grows at different rates and as as a function of its distance d from the energy source. The traces do not intersect, therefore, if we measure the charge pump output voltage at an early time, e.g, 30 ms as labeled in the picture, we can obtain a voltage across the reservoir capacitor $V_{\rm cap}$, with which we can predict the time required for the charge pump to fully (98%) charge C_1 —labeled as t_c in the measurement. For d from 10 cm to 50 cm, t_c takes an exponentially longer time. For operational range d>50 cm, the charge pump cannot accumulate energy to build up $V_{\rm cap}$; we even observed seldom loss of power. Notably, the MCU during our measurements is in a sleep state, while the charge pump, being an active device, itself consumes power to operate.

On the other hand, the time before brownout is also a function of d. We can observe in Fig.S4 (b), when d is less than 30 cm inclusive, the CRFID device can execute the MAC computation we employed for the load, continuously; starting form ta=110 ms without power failure. However, the device starts to fail or brown-out causing a power loss at t=142.92 ms, giving a time to brown out of $t_b=t_a+32.93$ ms for distance larger than 50 cm. As expected, we can see that t_b decreases as d increase.

$$\mathsf{PAM.Get}(Vt) = \begin{cases} [\infty, 0] &, & Vt \geq 2.393 \ V \\ [29.64 \ ms, 66.78 \ ms] &, & 2.393 \ V > Vt \geq 2.183 \ V \\ [13.71 \ ms, 76.66 \ ms] &, & 2.183 \ V > Vt \geq 2.143 \ V \\ [11.51 \ ms, 25 \ ms] &, & 2.143 \ V > Vt \geq 2.140 \ V \\ [9.39 \ ms, 25 \ ms] &, & Vt < 2.140 \ V \end{cases} \tag{3}$$

PAM function formulation. From our results, we can conclude: i) for d < 30 cm, where $Vt \geq 2.393$ V, the CRFID token may continuously operate with no power loss. In such cases, $t_{LPM} = 0$, and $t_{active} = \infty$ is used (execution does not need to be altered; ii) for Vt within 2.183 V and 2.393 V, we can employ $t_{LPM} = 66.78$ ms and $t_{active} = 29.64$ ms (90% the measured t_b) for a conservative approach to prevent power

⁷Notably, the RFID air interface relies on a slotted ALOHA media access control protocol.

TABLE SI. Comparing the Settings of Tokens

| Method | Pilot/Non-Overhearing role selection | Transponder mode | Ignore handle in SecureComm/ BlockWrite | SecureComm/ BlockWrite response | |
|-----------------------|--------------------------------------|------------------|---|---------------------------------------|--|
| Stork [12] | First seen by Host | Overhearing | / | × | |
| (insecure protocol) | riist seen by riost | non-Overhearing | × | ✓ | |
| Wisecr | The lowest Vt Token | Observer | ✓ | × | |
| (Our secure protocol) | THE towest vt Token | Pilot | × | ✓ | |

failures; iii) for Vt within 2.143 V and 2.183 V, use $t_{LPM} = 76.66$ ms and $t_{active} = 13.71$ ms; and iv) if $Vt \le 2.14$ V, then the CRFID device cannot accumulate adequate energy under such a condition to complete a computation intensive task, and we strongly suggest to not perform a code update in this case. We describe $(t_{active}, t_{LPM}) \leftarrow \mathsf{PAM.Get}(Vt)$ function in equation (3).

S VI. TRANSPONDER MODES AND BROADCAST CHANNEL

Stork [12] proposed exploiting promiscuous listening by choosing one in-field token (CRFID) to stay in the non-overhearing mode and the rest in overhearing (observer or promiscuous listening) mode to create a logical broadcast channel. This method overcomes the unicast media access layer protocol to facilitate wireless code dissemination to multiple CRFID devices. Building upon Stork, our Pilot-Observer mode (Section III.B.2) makes a key improvement. In contrast to Stork [12], for the token under Non-overhearing/Pilot mode, instead of selecting the first device responding to an interrogation signal from the Server, we elect the the device with the lowest reported voltage (V_t) as the pilot token. The similarties and differences between our work and the Stork are summarized in Table SI.

This method forces the broadcast session to be driven by the device with the lowest available energy, and the highest probability to brownout; thus, increasing the chance of all non responding tags remaining in synchronicity with the the processing of the broadcasted firmware, simply because these devices are able to harvest more power than the pilot token whilst also not having to respond to the Server.

S VII. COMPARISON WITH STORK (INSECURE METHOD)

We extensively compared the performance of our secure *Wisecr* scheme with Stork [12] method. Both aim to offer multiple CRFID wireless firmware updates, but no security is provided by Stork. Comparisons are carried out under three different test settings:

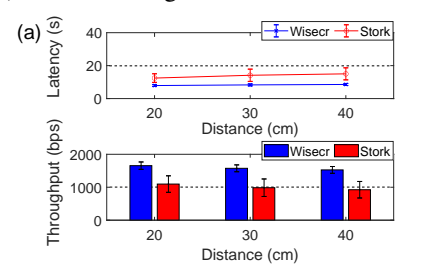
- Four different operating ranges from 20 to 50 cm.
- Updating 1 to 4 tags concurrently in-field to evaluate reduced latency to update (or improvements to scalability) (as in Stork, tags are at 20 cm from the antenna).

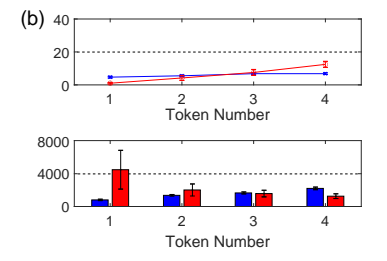
• Consider three different firmware sizes (as in Stork, tags are at 20 cm from the antenna).

We measured two performance metrics: i) latency; and ii) throughput as defined in Section V.A for each test setting. For both Stork and *Wisecr*, we used the same binary files generated from the same compilation. The settings in the *Wisecr* Server Toolkit are: 10 attempts per broadcast run; lowest voltage Vt_i pilot token selection method; Send Mode is set to Broadcast. Meanwhile, the settings in Stork are: BWPayload is set to throttle; Update Only is set to True; Reprogramming Mode is set to Broadcast; Compression is Disabled (as compression simply reduces the size of the firmware, we did not enable this option). All results are mean values reported from 100 repeated protocol update runs. Comparison results from our experiments are detailed in Fig.S5:

- From Fig. S5 (a): when powering channel state is reasonable i.e. from 20 cm to 40 cm, *Wisecr* outperforms Stork, as *Wisecr* does not need per-block checking and relies on the pilot token selection method to improve broadcast performance. However, Stork performs better than *Wisecr* at 50 cm when the powering channel condition is very poor because Stork is able to continue to transmit the firmware across power failures since the stork scheme does not need to meet any security requirements and therefore is able to send firmware payload in plaintext from the last correctly received payload. In contrast *Wisecr* gracefully fails when a power interruption cannot be prevented and all states (such as the session key) are lost and a new broadcast attempt must be made by the Server Toolkit.
- From Fig. S5 (b): *Wisecr* exhibits significantly better latency and throughput as the number of tokens increases.
- From Fig. S5 (c): both protocols show improved efficiency as larger payload/firmware sizes are transmitted. Notably, Wisecr exhibits much better efficiency attributed to the significantly reduced latency experienced during the broadcast method.

The gains in performance and faster updates to many devices achieved by *Wisecr* can be attributed to: i) our pilot token selection method to drive the protocol where a significantly large proportion of in-field tokens are updated in a single attempt; and ii) our validation method of complexity $O(n \cdot 1)$ where n is the number of tokens—although computationally intensive—is more lightweight than the read back mechanism of Stork, $O(n \cdot k)$ where k is the code size, relying on the narrow band communication channel employed by CRFID devices.





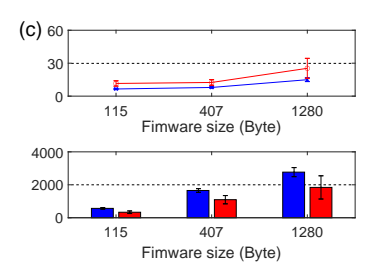


Fig. S5. We repeated the firmware update process for *Wisecr* (ours) and Stork to compare between Stork (providing *no security properties*) and our *Wisecr* scheme under three different test settings: (a) increasing operational range; (b) increasing number of tokens, and (c) payload sizes.